

國立清華大學

National Tsing Hua University

碩士論文

Master Thesis

低能有效框架下的玻色子：自子衰及更的束

Low Energy EFT Framework for Charged Boson Portals:

Constraints from Lepton Decays and Beyond

系別：物理系 Department of Physics

學號：110022421

研究生：黎德傳 Duc Truyen LE

指導教授：張維甫 We-Fu CHANG

中華民國一十二年一月

R.O.C. 112-10

# Abstract

This study presents a detailed construction of a low energy Effective Field Theory (EFT) framework that introduces novel charged bosons potentially deemed to be the SM and Dark sector portals. The newly charged mediators have coupling to photon and generally arbitrary couplings to fermions, both matter and dark matter particles, which therefore significantly contribute to hugely vast experimental processes. That adjusts the theoretical prediction of experimental values, particularly lepton decays within the scope of our study. Preliminary to this theoretical development is the verification of the anapole moment's disappearance at the one-loop order, guaranteeing its gauged invariant Lagrangian. By employing lepton decays, we impose constraints on the newly introduced couplings. A pivotal aspect of our analysis involves the use of Michel parameters [1, 2] derived from polarized muon decay, which plays a key role in assessing the chirality effects predicted by the theory. Our findings indicate that the proposed couplings are too constrained to explain the muon  $g-2$  anomaly if a universal coupling assumption is made. In addition, the given coupling pattern of UV models can also be applied to offer a better lower bound of detecting charged boson mass than collider searches that surpass and/or benchmarks with other current experimental searches.

Last but most importantly, the work addressed the rigorous constraints arising further from Lepton Flavor Violation decays and Neutrino Oscillation within the Zee Model context. Utilizing Michel parameters showcased an impactful point, which set out the comprehensive analysis of limiting parameter space for the Zee model to survive compared to other previous research works. The findings of this study provide a framework analysis for exploring new physics in the weak sector and offer a significant step forward in resolving longstanding anomalies in particle physics.

# Acknowledgements

To have the opportunity to complete this thesis and write such words here, I really want to say thank you all, who side by side have been supporting, helping, believing in me.

First of all, I would like to express my sincere gratitude to my supervisor, Prof. Chang We-Fu, who has supported me tremendously throughout both my student life and study path. Without his guidance, my achievements today would not have been possible. The professional knowledge and advice I have gained from him are invaluable, particularly in developing the physics insights and perspectives I lacked from my previous studies. His mentorship has been instrumental in helping me become more mature and sustainable in my research path. I genuinely want to say "thank you" to my dear teacher for being such an important part of my journey.

I am also grateful to Tsing Hua University for giving me the opportunity to work in such a renowned scientific environment, which was instrumental in accomplishing my thesis. Additionally, I would like to thank all the staff members of the Department of Physics for their thoughtful assistance. Special thanks go to my group members, Zhen-Yu and Shi-Xian, for their support, study discussions, and for sharing indelible moments together. My great time here has been enriched not only by professional growth but also by cultural exchanges and the vibrant student life, all of which I will cherish as lasting memories.

I take this opportunity to express gratitude to all of my teachers at the Department of Theoretical Physics: Prof. We-Fu, Yi-Ping, Kingman, Martin, Jennifer. Without their inspiring lectures, there might be not my passion today.

The last, to my parents, my family, who are always by my side, concern, believe, and favor me in the way of my dream of becoming a physicist. All my gratitude is not enough to describe their invaluable love for me, which makes me stronger every single day, dare to cope with all difficulties.



Tsingda, August 2024

Hsinchu city, Taiwan

**LE Duc Truyen**

# Contents

Abstract	I
Acknowledgements	II
Contents	IV
List of Figures	VI
List of Tables	VII
1 Introduction	1
2 Effective Field Theory model	3
2.1 Charged vector boson . . . . .	3
2.2 Charged scalar boson . . . . .	6
2.3 Feynman rule . . . . .	7
3 Muon decay	11
3.1 Michel parameters . . . . .	12
3.2 Fermi constant . . . . .	16
4 $L \rightarrow l\gamma$ decay process	17
4.1 Gauge invariant and Anapole vanishing . . . . .	17
4.1.1 Charged vector form factors . . . . .	19



4.1.2	Charged scalar form factors . . . . .	21
4.2	$L \rightarrow l\gamma$ and $(g - 2)_l$ . . . . .	23
4.2.1	$L \rightarrow l\gamma$ LFV decay . . . . .	23
4.2.2	$(g - 2)_l$ anomalous magnetics dipole moment . . . . .	24
<b>5</b>	<b>Coupling Constraints in muon decay experiments</b>	<b>28</b>
5.1	Case of universal coupling . . . . .	28
5.2	$a_l$ contributions from new charged bosons . . . . .	30
5.3	Case of non-universal coupling . . . . .	33
5.4	Coupling pattern from UV models . . . . .	36
<b>6</b>	<b>Constraints on Lepton Flavor Violation coupling applied to Extended Standard model Higgs sector</b>	<b>38</b>
6.1	Zee's model . . . . .	38
6.1.1	Universal test in Pion decay . . . . .	41
6.1.2	Neutrino Oscillation . . . . .	46
6.1.3	Trilepton decay constraint . . . . .	52
6.1.4	$L \rightarrow l\gamma$ . . . . .	55
6.1.5	Muon decay . . . . .	58
<b>7</b>	<b>Conclusion and Outlook</b>	<b>64</b>
<b>8</b>	<b>Appendix</b>	<b>66</b>
8.1	$L \rightarrow l\gamma$ form factor . . . . .	66
8.1.1	Charged vector form factors . . . . .	66
8.1.2	Charged scalar form factor . . . . .	71
8.2	Fierz transformation . . . . .	73
8.3	Full massive Lorenz index two-body phase pace . . . . .	74
	<b>Bibliography</b>	<b>76</b>

# List of Figures

4.1	$l_j \rightarrow l_i \gamma$ with new charged vector contribution . . . . .	19
4.2	$l_j \rightarrow l_i \gamma$ with new charged scalar contribution . . . . .	21
5.1	Yukawa couplings in muon parameters experiment values . . . . .	29
5.2	Vector couplings in muon experiment values . . . . .	30
5.3	Muon MDM values from new scalar's contribution in muon decay experiment's constrained region. . . . .	31
5.4	Muon MDM values from new vector's contribution in muon decay experiment's constrained region. . . . .	32
5.5	Electron MDM anomaly in the scalar's non-universality coupling . .	33
5.6	Muon MDM anomaly in the vector non-universality coupling . . . .	34
5.7	The new vector non-universality coupling's constraint . . . . .	35
5.8	2HDM constraint . . . . .	36

# List of Tables

5.1	2HDM type of couplings . . . . .	37
6.1	Trilepton decay constraints table . . . . .	54
6.2	Simple expression of Trilepton decay constraints . . . . .	55
6.3	Lep-to-lep-gamma constraints table . . . . .	58





# Chapter 1

## Introduction

In the quest to understand the fundamental constituents of nature, Effective Field Theory (EFT) has emerged as a powerful conceptual and mathematical framework, enabling physicists to systematically investigate the implications of these experimental findings. EFT allows physicists to focus on the relevant degrees of freedom at a given energy scale. In this work, instead of high-dimension operator encapsulating the physics in higher scale, we propose a low-energy EFT model that introduces a new charged boson. These particles are coupled in a manner that is renormalizable and invariant under  $U(1)_{\text{EM}}$  symmetry. The renormalizable coupling introduced here is designed to ensure that the new particles can be consistently incorporated into the EFT without introducing anomalies or breaking gauge invariance. This model serves as a benchmark and an applicable calculation framework for UV models broken down to the low-energy level.

Muon decay experiments provide some of the most precise measurements in particle physics, essential for probing fundamental phenomena and observables. Key quantities such as the Fermi constant [3], Michel parameters [4], and the anomalous magnetic moment of the muon ( $g-2$ ) [5] are crucial for testing the Standard Model (SM) and exploring new physics (NP) beyond it. The recent well-known discrepancy in the muon  $g-2$  measurement suggests potential new physics. The

new charged boson brought in to this study, either scalar or vector, takes action in the muon's decay, is aimed at resolving anomalies in the muon's weak interaction sector, and generalizes to other lepton weak processes. This EFT approach simplifies the parameter space and BSM operators, which predicts abundant phenomena as well as being a grounded benchmark for UV models with similar properties such as Sequential Standard Model, 2HDM, Zee model, etc. In the realm of Lepton Flavor Violation (LFV), the constraints placed by this study will guide future experiments and theories, potentially leading to novel discoveries or the refinement of existing models.

The structure of this thesis is as follows: Chapter 2 provides a detailed construction of EFT respecting the low-energy symmetry. Chapters 3 and 4 discuss the theoretical footings of the EFT underlying Michel parameters,  $g - 2$  and the leptonic decays's phenomenology study. The numerical study in Chapter 5, we yield the boundary constraint of new charged bosons and explore their potential solution for the  $g - 2$  problem via Michel parameters. Chapter 6 presents a detailed application of the Zee model, leveraging comprehensive studies of LFV decays along with neutrino oscillation data, we provide roughly estimated bounds for couplings and let here a promising parameter-constrained space for future study. Finally, Chapter 7 gives the conclusions and perspectives for future research.

# Chapter 2

## Effective Field Theory model

Departing from the call of new charged mediator playing a part in the lepton decays and potentially being able to reach in current experiment searches. Many UV models that entail newly charged bosons require a benchmark model on a low-energy scale. To address this, we employ the EFT approach, utilizing SM materials and introducing new charged bosons that respect the  $U(1)_{EM}$  group. This bottom-up approach, where we start with what we observe and carefully, piece by piece, build our model, in such a way that adheres to the given symmetries, by involving new fields and new adding-by-hand interaction terms, analogous to the Yukawa sector in the Standard Model. Apart from the typical approach in which we add non-renormalizable contributions along with the UV regulator  $\frac{1}{\Lambda}$ , where  $\Lambda$  is a new physics mass scale, herein, we introduce renormalizable couplings along between new particles and SM particles.

### 2.1 Charged vector boson

To construct an EFT Lagrangian with a new charged vector boson, we have to satisfy conventionally fundamental symmetries and invariances, at the low-energy scale, these are typically Lorentz invariance and  $U(1)_{EM}$  group. In the first step,

we bring in the kinetic term of charged vector field  $V_{\mu\nu}^{\pm} \equiv \partial_{\mu}V_{\nu}^{\pm} - \partial_{\nu}V_{\mu}^{\pm}$  in free interaction obeying Lorentz invariance

$$\mathcal{L}_{V^{\pm}} = \epsilon V_{\mu\nu}^{+} V^{-\mu\nu} + m^2 V_{\mu}^{+} V^{-\mu}, \quad (2.1)$$

where the factor magnitude is defined through E.O.M reduced to the Klein-Gordon equation

$$\partial_{\mu} \frac{\partial \mathcal{L}_{V^{\pm}}}{\partial (\partial_{\mu} V_{\nu}^{\pm})} - \frac{\partial \mathcal{L}_{V^{\pm}}}{\partial V_{\nu}^{\pm}} = 2a \partial^{\nu} V_{\mu\nu}^{\pm} + m^2 V_{\mu}^{\pm} = 0, \quad (2.2)$$

we obtain the Lorentz gauge condition  $\partial^{\mu} V_{\mu}^{\pm} = 0$  by taking derivative  $\partial^{\mu}$  to E.O.M. Consequently, to derive the relativistic Schrödinger equation for charged vector field, we set  $\epsilon = -\frac{1}{2}$

$$2\epsilon \partial^{\nu} (\partial_{\mu} V_{\nu}^{\pm} - \partial_{\nu} V_{\mu}^{\pm}) + m^2 V_{\mu}^{\pm} = (-2\epsilon \partial^{\nu} \partial_{\nu} + m^2) V_{\mu}^{\pm} = (\square + m^2) V_{\mu}^{\pm} = 0. \quad (2.3)$$

The relative sign between  $m^2$  and  $\epsilon$  is defined by the positive definite of energy

$$\mathcal{E} = \frac{\partial \mathcal{L}_{V^{\pm}}}{\partial (\partial_t V_{\mu}^{\pm})} \partial_t V_{\mu}^{\pm} - \mathcal{L}_{V^{\pm}} = -V^{\mp,0\mu} \partial_t V_{\mu}^{\pm} + \frac{1}{2} V_{\mu\nu}^{+} V^{-\mu\nu} - m^2 V_{\mu}^{+} V^{-\mu} \quad (2.4)$$

$$= \partial_i V_0^{\pm} \partial_0 V_i^{\mp} - \partial_i V_0^{+} \partial_i V_0^{-} - m^2 (V_0^{+} V_0^{-} - V_i^{+} V_i^{-}) \quad (2.5)$$

$$= (\partial_i V_0^{\pm} \partial_0 V_i^{\mp} + V_0^{\pm} \partial_0^2 V_0^{\mp}) - V_0^{\pm} (\square + m^2) V_0^{\mp} + m^2 V_i^{+} V_i^{-} \quad (2.6)$$

$$= m^2 V_i^{+} V_i^{-} \geq 0. \quad (2.7)$$

Here, we ignored the total derivative terms  $\partial_i \hat{\mathcal{O}}$  which has no effect on total energy after integration, and used the Klein-Gordon equation along with Lorentz gauge condition to extract Eq. 2.6 to Eq. 2.7. Indeed, the Lorentz gauge is used to constrain the Lorentz representation spin-zero component in the vector field, and in order to impose that such condition, the relative factor between  $\partial_{\mu} V_{\nu}^{\pm} \partial^{\mu} V^{\mp\nu}$  and  $\partial_{\mu} V_{\nu}^{\pm} \partial^{\nu} V^{\mp\mu}$  is fixed, subsequently,  $F_{\mu\nu}^{\pm}$  was then formed.

The second step involves interaction with the gauge field, especially photon, the standard procedure is that we convert the normal partial derivative to covariant derivative  $\partial_\mu \rightarrow D_\mu = \partial_\mu + ieQ_V A_\mu$ , the photon field  $A_\mu$  here basically played a role as an affine connection between two points in complex field space. Interestingly, it is not the end of our story, there is another photon interaction term that we can also include in our model, which basically exerts a contribution to the MDM effect

$$\mathcal{L}_{\text{int}} \supset aieQ_V F^{\mu\nu} V_\mu^+ V_\nu^-, \quad (2.8)$$

with factor  $\underline{a}$  is a “free” real number due to the antisymmetric photon field tensor  $F^{\mu\nu}$ . This is a mysterious emergence while we expected the full coupling with the photon field should be induced through the covariant derivative. In SM,  $V^\pm$  is indeed the  $W^\pm$  boson, and this bizarre effect originates from non-abelian properties and the connately neutral vector boson coming along with the charged one. To sustain the covariant derivative-based method and resolve the anomaly, hence, the neutral vector boson would do the job, nevertheless, we will not consider that and assume only the new charged boson appears. One more legit term is the quartic potential of  $V_\mu^\pm$ , such as  $b|V_\mu^\pm|^4$ , which we also ignored here thanks to its non-contribution to our relevant process.

Crucially, the coefficient  $\underline{a}$  in Eq. 2.8 must be fixed as a constant to ensure convergence of the magnetic dipole moment. The proper selection of  $\underline{a}$  avoids the divergence that would otherwise arise in the calculation of the MDM, a detailed address of this issue and proof within the context of this effective theory will be the subject of a discussion in Chapter 4. Therein, we will pinpoint the necessity of the contribution Eq. 2.8 for the renormalization of the MDM and its complementary role in the EFT framework, ensuring that the predictions of our model remain physically meaningful.

In the final step of our consideration, we formalize the interaction Lagrangian representing the dynamics between the charged vector bosons and the fermionic matter fields. This interaction is crucial, as it, in general, encapsulates the effects we aim to investigate, particularly those pertaining to the chiral properties of the weak force.

$$\mathcal{L}_{\text{int}} \supset \bar{\psi}_i \left( V_{ij}^L \hat{L} + V_{ij}^R \hat{R} \right) \gamma^\mu \psi_j V_\mu^- + \text{h.c.}, \quad (2.9)$$

where the couplings  $V_{ij}^L$  and  $V_{ij}^R$  represent the left-handed and right-handed interaction strengths, respectively, between fermions and the  $V^\pm$  boson. In the Standard Model, the right-handed coupling  $V_{ij}^R$  is absent, reflecting the purely left-handed nature of weak interactions. The introduction of a non-zero right-handed coupling signifies new physics that allows for right-handed currents. This chiral asymmetry is responsible for the observed parity violation in weak processes and could lead to discrepancies in weak interaction measurements if the right-handed terms contribute significantly.

The Lagrangian is constructed in generic form to reflect the potential chiral asymmetry from the UV models extended SM, for instance, the  $\text{SU}(3)_c \times \text{SU}(3)_L \times \text{U}(1)_X$  (331) model, Left-Right Symmetric Models (LRSM), Extra-Dimensional (ED) Models, or other GUTs models, topdown ultimately. Which is a novelty we unveiled, and sets the foundation for exploring the resulting phenomenological consequences.

## 2.2 Charged scalar boson

According to the same vision and procedure as we have done with the new charged vector, the Lagrangian for a new charged scalar boson is laid out below

$$\mathcal{L}_{\text{EFT}} \supset |D_\mu \phi|^2 - m_\phi^2 |\phi|^2 + \bar{\psi}_i \left( Y_{ij}^L \hat{L} + Y_{ij}^R \hat{R} \right) \psi_j \phi + \text{h.c.}, \quad (2.10)$$

differ from the charged vector case, information of photon interaction is completely encoded in covariant derivative  $D_\mu = \partial_\mu + ieQ_\phi A_\mu$  and interacting with fermion is described by the third term. Easy to see that the coefficients in Lagrangian are valid choices, in the sense both E.O.M and energy positive definite are satisfied. In free interaction, the E.O.M

$$\partial_\mu \frac{\partial \mathcal{L}_\phi}{\partial(\partial_\mu \phi^*)} - \frac{\partial \mathcal{L}_\phi}{\partial \phi^*} = (\square + m^2) \phi = 0, \quad (2.11)$$

and the energy density

$$\mathcal{E} = \frac{\partial \mathcal{L}_\phi}{\partial(\partial_t \phi^*)} (\partial_t \phi^*) - \mathcal{L}_\phi = |\partial_t \phi|^2 + |\vec{\nabla} \phi|^2 + m^2 |\phi|^2 \geq 0 \quad (2.12)$$

is positive definite. In Equation 2.8, the third term highlights our focus on experimental phenomenology, paralleling our approach in the charged vector case. This investigation delves into the effects within the weak interaction regime, a domain where each chiral type manifests distinct characteristics. From the context of EFT, this allows us to offer matching constraints to constraints of several UV models, which we'll briefly touch off in Chapter ?? through the lens of the experiment. Moreover, by leveraging our computational resources, we can effectively navigate the parameter space constraints of the triplet Higgs model.

## 2.3 Feynman rule

Here we souped up an Effective Lagrangian at the low-energy scale able to be all in one expressed in the following:

$$\mathcal{L}_{\text{EFT}} = \mathcal{L}_{\text{SM}} + \mathcal{L}_{\text{S}} + \mathcal{L}_{\text{Y}} + \mathcal{L}_{\text{F-V}^\pm} + \mathcal{L}_{\text{V}^\pm} + \mathcal{L}_\gamma, \quad (2.13)$$

Where  $\mathcal{L}_{\text{SM}}$  is the well-know SM Lagrangian, and each other parts are defined

$$\mathcal{L}_S = |D_\mu \phi|^2 - m_\phi^2 |\phi|^2, \quad (2.14)$$

$$\mathcal{L}_F = i\bar{\psi} \not{D}\psi - m_f^2 \bar{\psi}\psi, \quad (2.15)$$

$$\mathcal{L}_{V^\pm} = -\frac{1}{2}\tilde{V}_{\mu\nu}^+ \tilde{V}^{-\mu\nu} + m_V^2 V_\mu^+ V_\mu^- + ieQ_V a F^{\mu\nu} V_\mu^+ V_\nu^-, \quad (2.16)$$

$$\mathcal{L}_{F-S} = \bar{\psi}_i \left( Y_{ij}^L \hat{L} + Y_{ij}^R \hat{R} \right) \psi_j \phi + \text{h.c}, \quad (2.17)$$

$$\mathcal{L}_{F-V^\pm} = \bar{\psi}_i \left( V_{ij}^L \hat{L} + V_{ij}^R \hat{R} \right) \gamma^\mu \psi_j V_\mu^\pm + \text{h.c} \quad (2.18)$$

according to the  $U(1)_{\text{EM}}$  gauge transformation

$$\partial_\mu \rightarrow D_\mu = \partial_\mu + ieQ A_\mu \quad (2.19)$$

$$A_\mu \rightarrow A_\mu - \partial_\mu \alpha(x) \quad (2.20)$$

$$V_{\mu\nu}^- = \partial_\mu V_\nu^- - \partial_\nu V_\mu^- \rightarrow \tilde{V}_{\mu\nu}^- = D_\mu V_\nu^- - D_\nu V_\mu^- \quad (2.21)$$

$$\{\psi, \phi, V_\mu^\pm\} \rightarrow e^{ieQ\alpha(x)} \{\psi, \phi, V_\mu^\pm\}. \quad (2.22)$$

Be cautious, we assumed that either new charged vector or new charged scalar even though we wrote it in one line for simplification, but no interference between those. Couplings  $Y_{ij}^{R,L}, V_{ij}^{R,L}$  are complex element symmetric matrices such that their left-right relative phases are  $k\pi$  ( $k \in \mathbb{Z}$ ) for CP invariant condition, and  $a$  factor from an additional magnetic-moment contribution  $ieQ_V a F^{\mu\nu} V_\mu^+ V_\nu^-$  is purely real due to anti-symmetric of Electromagnetic Field Strength tensor  $F_{\mu\nu}$ . After investigating the Lepton-Flavor Violation (LFV) decay process  $L \rightarrow l\gamma$  where the EFT model takes a role, we will show that only  $a = 1$  for MDM/EDM renormalization. Note that, we did not include the new neutral boson here without violating any requirement from low-energy scale symmetry, while from the UV model, new charged bosons are inherently accompanied by new neutral bosons.

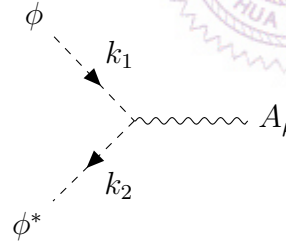
Moving forward, we've drawn up Feynman rules grounded in EFT Lagrangian



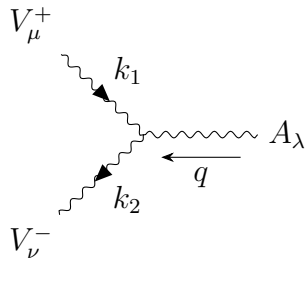
to serve as a point of reference for our ongoing work. We'll call on the peeling method to tease out the relevant formulas from the Lagrangian. The standard procedure [6] is

1. Lower (or raise) Lorentz index of the whole fields in all way same.
2. Replace all derivatives with the  $(-iq)$ , in which  $q$  is the incoming momenta of the fields they act on.
3. Sum up over all permutations of indices and momenta of identical external fields.
4. Shell out all external fields from consideration.

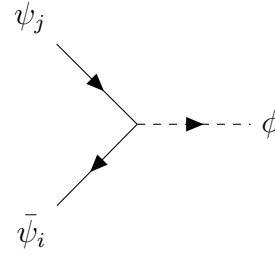
Where step 2 acts as a means to carry out the Fourier transformation, while steps 3 and 4 are tantamount to taking the derivative of the Lagrangian vertex. The Feynman rules from the new EFT fields are then called up beneath



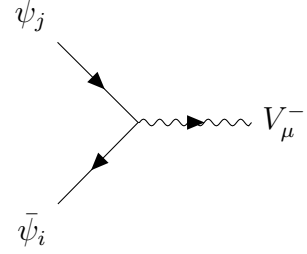
$$= -ieQ_\phi (k_1 + k_2)_\mu \quad (2.23)$$



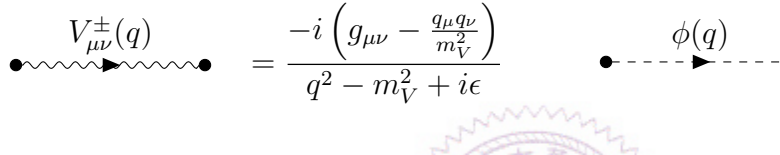
$$= -ieQ_V \left[ (k_2 - a.q)_\mu g_{\lambda\nu} + (k_1 + a.q)_\nu g_{\mu\lambda} - (k_1 + k_2)_\lambda g_{\mu\nu} \right] \quad (2.24)$$



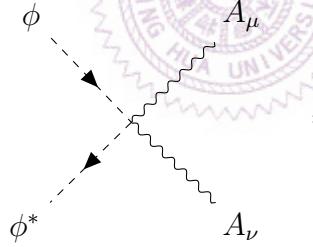
$$= i \left( Y_{ij}^L \hat{L} + Y_{ij}^R \hat{R} \right) \quad (2.25)$$



$$= i \left( V_{ij}^L \hat{L} + V_{ij}^R \hat{R} \right) \gamma_\mu \quad (2.26)$$



$$= \frac{-i \left( g_{\mu\nu} - \frac{q_\mu q_\nu}{m_V^2} \right)}{q^2 - m_V^2 + i\epsilon} = \frac{i}{q^2 - m_\phi^2 + i\epsilon} \quad (2.27)$$



$$= 2ie^2 Q_\phi^2 g_{\mu\nu} \quad (2.28)$$

The final Feynman rule is the representative quadratic photon interaction term of scalar QED, which is not relevant to our consideration. We let Eq. 2.24 in the generic form with the free factor  $\underline{a}$ . In SM, it will similarly cast the rule of the  $W^-$  boson as  $Q_V = -1$  and  $a = 1$ .

# Chapter 3

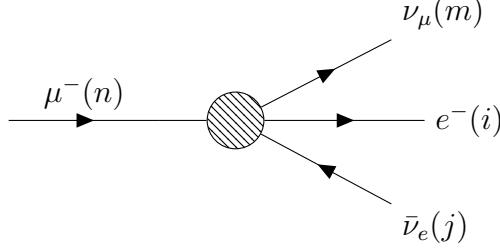
## Muon decay

Muon decay was measured at TRIUMF and PSI in the '80s with polarized muons from  $\pi$  decays that represent a cornerstone in the study of weak interactions, serving as a prototypical system for theoretical predictions and experimental validations in particle physics. The decay of polarized muons, in particular, offers a rich landscape for probing the underlying symmetries and mechanisms governing leptonic interactions. This investigation delves into the decay dynamics of muons within the framework of the new EFT model, exploring both the parity-nonconserving nature of weak forces and the implications of lepton universality.

The theoretical analysis herein is centered around a generalized formulation for the decay-electron distribution accommodateting polarized muon decay scenario by Michel parameters. By leveraging the polarization observables in muon decay, we aim to constrain the parameters governing weak interactions, offering insights into the validity of different theoretical constructs. This chapter is structured to initially delve into the theoretical foundation surrounding the decay parameter based on the EFT four-fermion interaction theory. This effort showcases the involvement of new physics (NP) in influencing experimental values, particularly focusing on the consequences these parameters have in polarized muon decays. Subsequently, we probe the detectable impact of NP on the Fermi constant by

considering the muon lifetime.

### 3.1 Michel parameters



The point-like interaction in muon decay is governed by the 4-Fermi theory that is matched to the EFT couplings by the Fierz transformation. In this way, we study Michel parameters from the muon decay process to make constraints on the new couplings, and calculations in this chapter are generally able to apply to all other fermion decay modes if the massless of the final states is supposed. The differential decay rate of the muon is in the form:

$$d\Gamma = \frac{m_\mu^5}{3 * 2^9 * \pi^4} * (a + 4b + 6c) \left\{ 3(1-x) + 2\rho \left( \frac{4}{3}x - 1 \right) - \xi \cos \theta \left[ (1-x) + 2\delta \left( \frac{4}{3} - 1 \right) \right] \right\} x^2 dx, \quad (3.1)$$

where  $\rho, \xi, \delta$  are Michel parameters [1] measured from experiment, which are defined [2]

$$\rho = \frac{3b + 6c}{a + 4b + 6c} \quad (3.2)$$

$$\delta = \frac{3b' - 6c'}{-3a' + 4b' - 14c'} \quad (3.3)$$

$$\xi = \frac{3a' - 4b' + 14c'}{a + 4b + 6c}. \quad (3.4)$$

Herein, we assumed the zero mass of outgoing particles, that caused suppression of the Michel parameter associated to the electron mass  $\eta$  [7]. In Eq. 3.1, the lepton-number nonconservation is not possible to detect in muon decay, and these

two parameters  $\delta, \xi$  merely contribute to emitted electron distribution angle. The full treatment of the massive final state's phase space, which is useful for studying the effect of Dirac and Majorana neutrino mass in Michel parameters, is performed calculations in Appendix 8.

Note that, we consider either case, only a new scalar or new vector, where the coupling combinational parameters are defined in the new scalar case

$$a = \frac{|Y_{ij}^L Y_{nm}^{R*}|^2 + |Y_{ij}^R Y_{nm}^{L*}|^2}{16m_\phi^4} \quad (3.5)$$

$$a' = \frac{|Y_{ij}^L Y_{nm}^{R*}|^2 - |Y_{ij}^R Y_{nm}^{L*}|^2}{16m_\phi^4} \quad (3.6)$$

$$b = \frac{|Y_{ij}^L Y_{nm}^{L*}|^2 + |Y_{ij}^R Y_{nm}^{R*}|^2}{16m_\phi^4} + \frac{g^4}{16m_W^4} \quad (3.7)$$

$$b' = \frac{|Y_{ij}^R Y_{nm}^{R*}|^2 - |Y_{ij}^L Y_{nm}^{L*}|^2}{16m_\phi^4} + \frac{g^4}{16m_W^4} \quad (3.8)$$

$$c = \frac{|Y_{ij}^L Y_{nm}^{R*}|^2 + |Y_{ij}^R Y_{nm}^{L*}|^2}{32m_\phi^4} \quad (3.9)$$

$$c' = \frac{|Y_{ij}^R Y_{nm}^{L*}|^2 - |Y_{ij}^L Y_{nm}^{R*}|^2}{32m_\phi^4}, \quad (3.10)$$

or in the new vector mediator

$$a = \frac{|V_{ij}^L V_{nm}^{R*}|^2 + |V_{ij}^R V_{nm}^{L*}|^2}{m_V^4} \quad (3.11)$$

$$a' = \frac{|V_{ij}^L V_{nm}^{R*}|^2 - |V_{ij}^R V_{nm}^{L*}|^2}{m_V^4} \quad (3.12)$$

$$b = \frac{|V_{ij}^L V_{nm}^{L*}|^2 + |V_{ij}^R V_{nm}^{R*}|^2}{4m_\phi^4} + \frac{g^4}{16m_W^4} + \frac{g^2}{4m_W^2 m_V^2} \text{Re}(V_{ij}^R V_{nm}^{R*}) \quad (3.13)$$

$$b' = \frac{|V_{ij}^R V_{nm}^{R*}|^2 - |V_{ij}^L V_{nm}^{L*}|^2}{4m_\phi^4} + \frac{g^4}{16m_W^4} + \frac{g^2}{4m_W^2 m_V^2} \text{Re}(V_{ij}^R V_{nm}^{R*}) \quad (3.14)$$

are in terms of coupling parameters that we are going to constrain. Because of

$|a'| \leq a, |b'| \leq b, |c'| \leq c$ , these below inequalities always hold [4]

$$|\xi\delta| \leq \rho, \quad (3.15)$$

$$0 \leq \rho \leq 1, \quad (3.16)$$

and

$$0 \leq |\xi| \leq 3 - \frac{2}{3}\rho. \quad (3.17)$$

The symmetry and anti-symmetry between left-right couplings are encoded in  $\rho$  and  $\delta$  respectively, particularly non-prime and prime parameters. Consequently, if only one chirality gets in that will turn out the same behavior, say, the predicted value  $\rho = \delta = \frac{3}{4}$  same as Standard Model, and then constrain  $|\xi| \leq 1$ . The relative left-right difference effect is ascribed to  $\xi$ , which gives rise to changes in the angle of electron distribution. And if the true experiment turns out  $|\xi| \geq 1$ , it is definitely a hint of new physics involving both left-right interactions, at least in the vector boson sector or the lepton number violation interaction in the Yukawa sector.

As long as the neutrinos are massless and unobserved, the scalar case is non-sensitive to the LFV process on account of the non-interference between spin-0 (new scalar) and spin-1 (W boson), while this effect is characterized by the new vector case through the overlapped term.

To simplify, we further assume the universality and diagonal properties of the coupling parameters matrix, and then our case is reduced to

- For scalar case

$$a = \frac{|Y^L|^2 |Y^R|^2}{8m_\phi^4} \quad (3.18)$$

$$a' = 0 \quad (3.19)$$

$$b = \frac{|Y^L|^4 + |Y^R|^4}{16m_\phi^4} + \frac{g^4}{16m_W^4} \quad (3.20)$$

$$b' = \frac{|Y^R|^4 - |Y^L|^4}{16m_\phi^4} + \frac{g^4}{16m_W^4} \quad (3.21)$$

$$c = \frac{|Y^L|^2 |Y^R|^2}{64m_\phi^4} \quad (3.22)$$

$$c' = 0. \quad (3.23)$$

- For vector case

$$a = 2 \frac{|V^L|^2 |V^R|^2}{m_V^4} \quad (3.24)$$

$$a' = 0 \quad (3.25)$$

$$b = \frac{|V^L|^4 + |V^R|^4}{4m_V^4} + \frac{g^4}{16m_W^4} + \frac{g^2}{4m_W^2 m_V^2} |V^R|^2 \quad (3.26)$$

$$b' = \frac{|V^R|^4 - |V^L|^4}{4m_V^4} + \frac{g^4}{16m_W^4} + \frac{g^2}{4m_W^2 m_V^2} |V^R|^2. \quad (3.27)$$

The SM-like coupling means giving no deviation from SM contribution of Michel parameters, which are in the situation of only  $Y^L$  and  $V^R$  being involved, will be unbounded by the Michel parameters experiment as those are in sets of SM value prediction  $\rho = \delta = \frac{3}{4}, \xi = -1$ . As is straightforward to the eye, the universality condition implies the  $\delta = \frac{3}{4}$ .

## 3.2 Fermi constant

Integrating Eq. (3.1) over outgoing electron energy, the Muon decay rate is obtained

$$\Gamma = \frac{m_\mu^5}{3 * 2^9 * \pi^3} (a + 4b + 6c) = \frac{m_\mu^5 G_F^{\mu^2}}{192\pi^3}, \quad (3.28)$$

we then are able to extract the Fermi constant in terms of new coupling constants

$$(a + 4b + 6c) = 8G_F^{\mu^2}. \quad (3.29)$$

Because the lifetime of the muon is well-measured, which is thus, by far, the best determination of the Fermi constant  $G_F^\mu$ , and in fact, it is more than 100 times better than the other independent determination methods. In the new model scenario, the new physics positively contributes to the Fermi constant, which makes the value larger than the SM contribution. Since the new charged currents are in consideration, thus, an independent determination of the Fermi constant from the neutral current, which is in this report extracted from Z boson decay  $G_F^Z$ , can help to bound the allowable region of new coupling magnitudes. Furthermore, the tension between independent determinations of  $G_F$ , such as electroweak fits,  $\mu$ -decay, and CKM unitary are potentially resorted to setting a stringent NP constraint via the Standard Model EFT (SMEFT) approach [3].



# Chapter 4

## $L \rightarrow l\gamma$ decay process

In this chapter follow, we will delve deep into the heart of this lep-to-lep-gamma process, exploring its significance and physics implications through the lens of Feynman diagram calculations and analytical dissections. This study takes us to a deeper understanding and extracts results of Magnetic Dipole Moment (MDM) and the Lepton Flavour Violation (LFV) decay  $L \rightarrow l\gamma$ , then profoundly demonstrates the anomaly-free of gauge invariance of the EFT model through vanishing anapole, whose exploration is crucial for the validation of our theory. Moreover, as a progress, we will also uncover the indispensable role of extra photon coupling in contributing to the MDM of the charged vector models.

### 4.1 Gauge invariant and Anapole vanishing

Using  $\mathcal{L}_{\text{EFT}}$  above to investigate the contribution to the LFV decay, that consists of all possible leading effects which only come from scalar field  $\phi$  and vector field  $V_\mu^\pm$  mediator. The matrix element for the process  $l_j \rightarrow l_i\gamma$  emitting a real photon  $\mathcal{M}^\mu = \bar{u}_i(p)\Gamma^\mu u_j(p+q)$ , the interaction vertex  $\Gamma^\mu$  can be formally decomposed

into form factors

$$\Gamma^\mu(q^2 = 0) = \gamma^\mu F_1 + \gamma^\mu \gamma_5 G_1 + i\sigma^{\mu\nu} q_\nu F_2 + i\sigma^{\mu\nu} q_\nu \gamma_5 G_2, \quad (4.1)$$

where  $F_1, G_1$  associated to  $\gamma^\mu$  are Dirac and Anapole form factors, gauge invariance property enforces  $G_1 = 0$  though;  $F_2, G_2$  associated to  $\sigma^{\mu\nu} q_\nu$  are Magnetic Dipole (MDM) and Electric Dipole Moment (EDM) respectively. To universal interactions from the EFT Lagrangian are charged scalar  $\phi$  and vector  $V^\pm$  considered separately, where

$$F_1(G_1) = \sum_i^{[a,b,c,d]} F_1^{\phi,i} (G_1^{\phi,i}) + \sum_i^{[a,b,c,d]} F^{V,i} (G_1^{V,i}) \quad (4.2)$$

$$F_2(G_2) = \sum_i^{[a,b,c,d]} F_2^{\phi,i} (G_2^{\phi,i}) + \sum_i^{[a,b,c,d]} F^{V,2} (G_2^{V,i}) \quad (4.3)$$

we sum  $\sum_i^{[a,b,c,d]}$  overall diagram contributions of each class and represent them by Passarino-Veltman (PV) convention functions [6, 8, 9]

$$C_{i,j,\dots}^{V(\phi),a} = C_{i,j,\dots}^{V(\phi),a} (m_2^2, 0, m_1^2, m_k, m_{V(\phi)}, m_{V(\phi)}) \quad (4.4)$$

$$C_{i,j,\dots}^{V(\phi),d} = C_{i,j,\dots}^{V(\phi),d} (m_2^2, 0, m_1^2, m_{V(\phi)}, m_k, m_k) \quad (4.5)$$

$$B_{i,j,\dots}^{V(\phi),b} = B_{i,j,\dots}^{V(\phi),b} (m_1^2, m_k, m_{V(\phi)}) \quad (4.6)$$

$$B_{i,j,\dots}^{V(\phi),b} = B_{i,j,\dots}^{V(\phi),b} (m_2^2, m_k, m_{V(\phi)}) \quad (4.7)$$

fully expressed form factors in terms of PV function are found in Appendix 8. Expanding the exact calculation of PV functions, we showed that  $F_1 = G_1 = 0$ , that means  $\gamma^\mu$  terms vanish in the  $l_i \rightarrow l_j + \gamma$  decay process described by generic EFT Lagrangian Eq. (2.13). Under CP transformation, the EDM  $G_2$  term  $\bar{\psi} \sigma_{\mu\nu} \gamma_5 F^{\mu\nu} \rightarrow -\bar{\psi} \sigma_{\mu\nu} \gamma_5 F^{\mu\nu}$  is non-invariant, which presumably are hints stemming from higher symmetry CP violation sources. As tangibly, the interaction terms

in Eq. 2.13 encoded the higher symmetry model, which in general can be non-CP conserved. On the other side, the anapole term  $G_1$  is not only P violated but also does not preserve gauge invariance, thus, anapole inevitably vanishes in the gauge invariant theory, otherwise the EFT theory is incomplete. In the classical regime, where the gauge invariant Lagrangian became obvious, to ascertain if there is not an anomaly in our model, checking gauge invariant in the loop level contribution is conducted, which is verified through satisfying Ward Identity

$$q_\mu \Gamma^\mu(q^2 = 0) = \not{q} F_1(q^2 = 0) + \not{q} \gamma_5 G_1(q^2 = 0) = 0 \quad (4.8)$$

with on-shell ( $q^2 = 0$ ) photon four-momentum. In case of LFV decay, or  $l_j \neq l_i$ , both  $F_1(q^2 = 0) = G_1(q^2 = 0) = 0$  conditions are obligated to satisfy. We are henceforth employing the assumption of a heavy charged boson  $m_{V,\phi} \gg m_l$  and taking the approximated expansion at order  $\mathcal{O}\left(\frac{m_l^2}{m_{V,\phi}^2}\right)$  for simplicity.

#### 4.1.1 Charged vector form factors

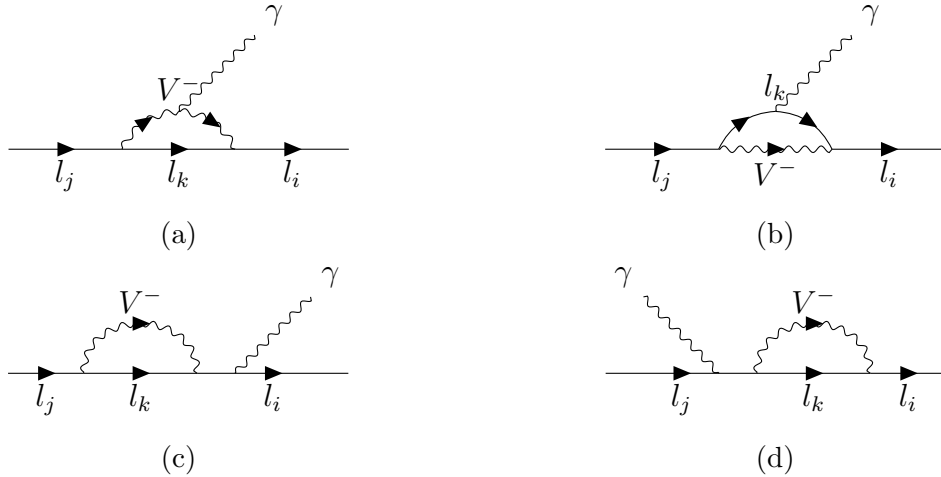


Figure 4.1:  $l_j \rightarrow l_i \gamma$  with new charged vector contribution

1.

$$G_1^{V,a} = \frac{eQ_V}{24} \left\{ \left( V_L^{*ki} V_L^{kj} - V_R^{*ki} V_R^{kj} \right) \left[ \frac{6(m_j^2 - m_j m_i + m_i^2 - 3m_k^2)}{m_V^2} \left( \frac{1}{\epsilon} + \log \left[ \frac{\mu^2}{m_V^2} \right] \right) \right. \right. \\ \left. \left. - 18 + \frac{(7m_j^2 - 7m_j m_i + 7m_i^2 - 33m_k^2)}{m_V^2} \right] + \left( V_L^{*ki} V_R^{kj} - V_R^{*ki} V_L^{kj} \right) \frac{18(m_i - m_j) m_k}{m_V^2} \right\} \quad (4.9)$$

2.

$$G_1^{V,b} = \frac{eQ_k}{24} \left\{ \left( V_L^{*ki} V_L^{kj} - V_R^{*ki} V_R^{kj} \right) \left[ \frac{6(m_j^2 - m_j m_i + m_i^2 - 3m_k^2)}{m_V^2} \left( \frac{1}{\epsilon} + \log \left[ \frac{\mu^2}{m_V^2} \right] \right) \right. \right. \\ \left. \left. - 18 + \frac{(7m_j^2 - 7m_j m_i + 7m_i^2 - 33m_k^2)}{m_V^2} \right] + \left( V_L^{*ki} V_R^{kj} - V_R^{*ki} V_L^{kj} \right) \frac{18(m_i - m_j) m_k}{m_V^2} \right\} \quad (4.10)$$

3.

$$G_1^{V,c} = \frac{eQ_l}{4(m_i + m_j)} \left\{ m_j \left( V_L^{*ki} V_L^{kj} - V_R^{*ki} V_R^{kj} \right) \left[ \left( \frac{m_j^2 - 3m_k^2}{m_V^2} \right) \left( \frac{1}{\epsilon} + \log \left[ \frac{\mu^2}{m_V^2} \right] \right) - 3 \right. \right. \\ \left. \left. + \frac{(7m_j^2 - 33m_k^2)}{6m_V^2} \right] + \left( Y_L^{*ki} Y_R^{kj} - Y_R^{*ki} Y_L^{kj} \right) \left[ \left( 6m_k + 6\frac{m_k^3}{m_V^2} \right) \left( \frac{1}{\epsilon} + \log \left[ \frac{\mu^2}{m_V^2} \right] \right) \right. \right. \\ \left. \left. + 2m_k - \frac{m_k(3m_j^2 + 2m_k^2)}{m_V^2} \right] \right\} \quad (4.11)$$

4.

$$G_1^{V,d} = \frac{eQ_l}{4(m_i + m_j)} \left\{ m_i \left( V_L^{*ki} V_L^{kj} - V_R^{*ki} V_R^{kj} \right) \left[ \left( \frac{m_i^2 - 3m_k^2}{m_V^2} \right) \left( \frac{1}{\epsilon} + \log \left[ \frac{\mu^2}{m_V^2} \right] \right) - 3 \right. \right. \\ \left. \left. + \frac{(7m_i^2 - 33m_k^2)}{6m_V^2} \right] - \left( V_L^{*ki} V_R^{kj} - V_R^{*ki} V_L^{kj} \right) \left[ \left( 6m_k + 6\frac{m_k^3}{m_V^2} \right) \left( \frac{1}{\epsilon} + \log \left[ \frac{\mu^2}{m_V^2} \right] \right) \right. \right. \\ \left. \left. + 2m_k - \frac{m_k(3m_i^2 + 2m_k^2)}{m_V^2} \right] \right\} \quad (4.12)$$

The absence of the parameter  $\underline{a}$  indicates that the additional interaction term in-

volving the photon and the newly introduced charged vector does not get part in this form factor, therefore solely influencing the MDM/EDM. The pattern explicitly presents how the diagram's anapole form factor contributions are rooted out to preserve the gauged invariance.  $\frac{G_1^{V,c}+G_1^{V,d}}{Q_l} = \frac{G_1^{V,b}}{Q_V} = \frac{G_1^{V,a}}{Q_k}$  corresponds to terms proportional to  $(V_L^{*ki}Y_L^{kj} - V_R^{*ki}Y_R^{kj})$  and UV finite of  $(V_L^{*ki}V_R^{kj} - V_R^{*ki}V_L^{kj})$  terms, meanwhile UV divergence in  $(V_L^{*ki}V_R^{kj} - V_R^{*ki}V_L^{kj})$  terms pertaining to  $G_1^{V,c}$  and  $G_1^{V,d}$  form factors canceling out each others. That manifestly combinatorial each other subtracting off even in  $l_i = l_j$  case, which brings the Ward Identity  $q_\mu \bar{u}_i \Lambda^\mu (q^2 = 0) u_i = \bar{u}_i \not{q} \gamma_5 G_1 \bar{u}_i = 0$  about to be obeyed. Otherwise, the Dirac form factor in the same expression within replacing  $m_j \rightarrow -m_j$  and  $V_L^{kj} \rightarrow -V_L^{kj}$ , which however strikes divergence as  $l_i = l_j$ , but this divergence can be resolved through the application of the renormalization technique nonetheless.

#### 4.1.2 Charged scalar form factors

In place of discussing anapole terms, we will illustrate the cancellation of the Dirac term as  $m_i \neq m_j$ , and the behavior of the anapole will be similarly followed.

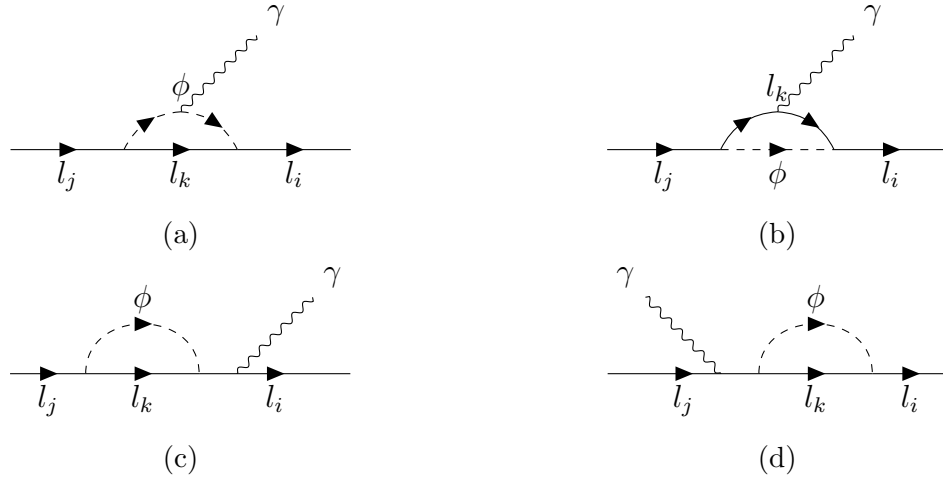


Figure 4.2:  $l_j \rightarrow l_i \gamma$  with new charged scalar contribution

1.

$$F_1^{\phi,a} = \frac{eQ_\phi}{8} \left\{ \left( Y_L^{*ki} Y_L^{kj} + Y_R^{*ki} Y_R^{kj} \right) \left[ 2 \left( \frac{1}{\epsilon} + \log \left[ \frac{\mu^2}{m_\phi^2} \right] \right) + 1 \right. \right. \\ \left. \left. + \frac{2(m_j^2 + m_j m_i + m_i^2 - 3m_k^2)}{3m_\phi^2} \right] + 2 \left( Y_L^{*ki} Y_R^{kj} + Y_R^{*ki} Y_L^{kj} \right) \frac{(m_i + m_j) m_k}{m_\phi^2} \right\} \quad (4.13)$$

2.

$$F_1^{\phi,c} = \frac{eQ_l}{8(m_j - m_i)} \left\{ m_j \left( Y_L^{*ki} Y_L^{kj} + Y_R^{*ki} Y_R^{kj} \right) \left[ 2 \left( \frac{1}{\epsilon} + \log \left[ \frac{\mu^2}{m_\phi^2} \right] \right) - \frac{2(m_j^2 - 3m_k^2)}{3m_\phi^2} + 1 \right] \right. \\ \left. + 4 \left( Y_L^{*ki} Y_R^{kj} + Y_R^{*ki} Y_L^{kj} \right) \left[ \left( m_k - \frac{m_k^3}{m_\phi^2} \right) \left( \frac{1}{\epsilon} + \log \left[ \frac{\mu^2}{m_\phi^2} \right] \right) + m_k - \frac{m_k(m_j^2 + 2m_k^2)}{2m_\phi^2} \right] \right\} \quad (4.14)$$

3.

$$F_1^{\phi,d} = \frac{eQ_l}{8(m_i - m_j)} \left\{ m_i \left( Y_L^{*ki} Y_L^{kj} + Y_R^{*ki} Y_R^{kj} \right) \left[ 2 \left( \frac{1}{\epsilon} + \log \left[ \frac{\mu^2}{m_\phi^2} \right] \right) - \frac{2(m_i^2 - 3m_k^2)}{3m_\phi^2} + 1 \right] \right. \\ \left. + 4 \left( Y_L^{*ki} Y_R^{kj} + Y_R^{*ki} Y_L^{kj} \right) \left[ \left( m_k - \frac{m_k^3}{m_\phi^2} \right) \left( \frac{1}{\epsilon} + \log \left[ \frac{\mu^2}{m_\phi^2} \right] \right) + m_k - \frac{m_k(m_i^2 + 2m_k^2)}{2m_\phi^2} \right] \right\} \quad (4.15)$$

4.

$$F_1^{\phi,b} = \frac{eQ_k}{8} \left\{ \left( Y_L^{*ki} Y_L^{kj} + Y_R^{*ki} Y_R^{kj} \right) \left[ 2 \left( \frac{1}{\epsilon} + \log \left[ \frac{\mu^2}{m_\phi^2} \right] \right) + 1 \right. \right. \\ \left. \left. + \frac{2(m_j^2 + m_j m_i + m_i^2 - 3m_k^2)}{3m_\phi^2} \right] + 2 \left( Y_L^{*ki} Y_R^{kj} + Y_R^{*ki} Y_L^{kj} \right) \frac{(m_i + m_j) m_k}{m_\phi^2} \right\} \quad (4.16)$$

Equivalent to the charged vector case, from the above expressions,  $F_1^{\phi,c} + F_1^{\phi,d} \propto F_1^{\phi,b} \propto F_1^{\phi,a}$  in such terms accompanied by  $(Y_L^{*ki} Y_L^{kj} + Y_R^{*ki} Y_R^{kj})$ , respectively

propositional to their own particle's charge emitting photon. They all sum up to zero if we impose  $Q_l + Q_\phi + Q_k = 0$ . In the  $\left(Y_L^{*ki}Y_R^{kj} + Y_R^{*ki}Y_L^{kj}\right)$  terms, both  $F_1^{\phi,c}$  and  $F_1^{\phi,d}$  offset UV divergent parts of each other, and then the UV finite part of  $F_1^\phi$  of altogether vanish if charge conversation is held on. The same conclusion for anapole form factors  $G_1^\phi$  in expressions substituted  $F_1^\phi$  by  $m_j \rightarrow -m_j$  and  $Y_L^{kj} \rightarrow -Y_L^{kj}$ .

## 4.2 $L \rightarrow l\gamma$ and $(g - 2)_l$

The ongoing dialogue between theoretical predictions and experimental measurements in the realm of the lepton  $g - 2$  and flavor violation decay, particularly muon, continues to be a fertile ground for discovering new physics. The measurement of the muon's anomalous magnetic moment  $a_\mu$  thus remains a key focus in high-energy physics, symbolizing the intricate interplay between theoretical innovation and empirical validation.

Meanwhile, EFT models can potentially provide insights into the scale and nature of new physics that could account for the measuremental values, allowing for bridging the gap between the currently observed phenomena in the MDM/LFV measurements and the enormous of possible explanations of underlying theoretical framework, paving the way for a deeper understanding of fundamental physics. This not only aids in pinpointing the specific nature of the new interactions or particles but also helps in guiding future experimental searches.

### 4.2.1 $L \rightarrow l\gamma$ LFV decay

In the intriguing landscape of particle physics, LFV decay stands out as a phenomenon that defies the Standard Model's predictions, offering a window into potential new physics. The parity of these decays, in which a lepton of one fla-

vor, such as a muon, transforms into another, like an electron, without conserving flavor, has fueled extensive theoretical speculation. Various models attempting to account for LFV have emerged, each proposing novel mechanisms and particles beyond the Standard Model, such as models addressing massive neutrinos, leptoquark (LQ) model, R-parity violating supersymmetry, etc. Amidst these diverse theoretical constructs, EFT plays on a bottom-up approach, which provides a versatile framework, enabling physicists to systematically analyze LFV processes without committing to a specific underlying theory smoothing the path for a deeper understanding of these rare decays.

Eq .4.1 tells us how to perform the calculation of the LFV decay rate

$$i\mathcal{M}_\nu = \bar{l}_i(k_i) \sigma^{\mu\nu} (F_2 + G_2\gamma_5) l_j(k_j) q_\mu \quad (4.17)$$

where  $q = k_j - k_i$  is the on-shell emitting photon four-momentum. Assuming that the heavy mass of decaying particle  $m_j \gg m_i$  we then derive the decay rate

$$\Gamma(l_j \rightarrow l_i \gamma) = \frac{m_j^3}{8\pi} (|F_2|^2 + |G_2|^2), \quad (4.18)$$

in which the squared amplitude and two-body phase space used are the following

$$|\mathbf{M}|^2 = 4m_j^4 (|F_2|^2 + |G_2|^2) \quad (4.19)$$

$$\int dP_2 = \int \frac{d^3 k_i}{2k_i^0 (2\pi)^3} \frac{d^3 q}{2q^0 (2\pi)^3} (2\pi)^4 \delta^4(k_j - k_i - q) = \frac{\pi}{2}. \quad (4.20)$$

### 4.2.2 $(g - 2)_l$ anomalous magnetic dipole moment

The measurement of the muon's anomalous magnetic moment denoted as  $(g - 2)$ , stands as a cornerstone in precision particle physics and probes the frontiers of



the Standard Model. Achieving sub-parts-per-million (ppm) precision, this measurement offers a window into physics beyond the Standard Model. The muon magnetic dipole moment, expressed as  $\vec{\mu} = ge\frac{e}{2m}\vec{S}$ , where  $\vec{S}$  is the muon's spin angular momentum, is foundational to these explorations, Dirac exactly predicted by his equation  $g = 2$  in the classical limit, and then Schwinger derived  $a_\mu \equiv \frac{(g-2)_\mu}{2} = \frac{\alpha}{2\pi}$  in QED first order quantum correction. Recent experimental results, particularly from the Fermilab Muon  $g - 2$  experiment, have corroborated earlier findings from the Brookhaven National Laboratory, intensifying the  $4.2\sigma$  discrepancies between experimental data and Standard Model predictions.

On the theoretical front, efforts to reconcile these discrepancies have been robust. Theoretical physicists have proposed various extensions to the Standard Model, such as supersymmetry, leptoquarks, and dark photons, as potential explanations for the observed anomaly. These models introduce new particles or interactions that could contribute to the muon  $g - 2$  value, thus potentially resolving the tension between theory and experiment. Moreover, refined calculations incorporating quantum electrodynamics, hadronic contributions, and electroweak interactions have been performed, offering nuanced insights into the muon's behavior. These theoretical updates are critical for enhancing our understanding of fundamental physics, providing new directions for theoretical exploration and experimental verification.

As is customary, the EFT model proposed embarks on the game to lay on a preliminary robust stone that bridges to the higher-scale UV theories. The MDM/EDM form factor formulated in Eq. 4.1 is useful to acquire LFV decay rate

Eq. 4.18 as well, newly charged scalar and vector contribution are<sup>1</sup>

$$F_2^\phi = \frac{-e}{3.27 m_\phi^2 \pi^2} \left[ (m_i + m_j) (Q_\phi - 2Q_k) \left( Y_L^{*ki} Y_L^{kj} + Y_R^{*ki} Y_R^{kj} \right) \right. \\ \left. + 6m_k \left( Q_\phi + 3Q_k + 2Q_k \log \left[ \frac{m_k^2}{m_\phi^2} \right] \right) \left( Y_L^{*ki} Y_R^{kj} + Y_R^{*ki} Y_L^{kj} \right) \right] \quad (4.21)$$

and

$$F_2^V = \frac{e}{3.27 m_V^2 \pi^2} \left[ (m_i + m_j) (Q_V - 8Q_k + 9aQ_V) \left( V_L^{*ki} V_L^{kj} + V_R^{*ki} V_R^{kj} \right) \right. \\ \left. - 6m_k (5a - 1) Q_V \left( V_L^{*ki} V_R^{kj} + V_R^{*ki} V_L^{kj} \right) \right] + (a - 1) \frac{eQ_V}{2^6 m_V^2 \pi^2} \times \\ \left[ \left( V_L^{*ki} V_L^{kj} + V_R^{*ki} V_R^{kj} \right) (m_i + m_j) - 2m_k \left( V_L^{*ki} V_R^{kj} + V_R^{*ki} V_L^{kj} \right) \right] \left( \frac{1}{\epsilon} + \log \left[ \frac{\mu^2}{m_V^2} \right] \right). \quad (4.22)$$

As mentioned earlier, the quantity  $F_2^V$  exhibits UV divergence apparently popping up in Eq. 4.22 unless  $a = 1$ . This critical function of the extra adding-by-hand ED interaction term in the charged vector sector physicalizes  $F_2^V$  to meaningful experimental prediction. Within UV theories like SM, that additional term  $aieQ_V F^{\mu\nu} V_\mu^+ V_\nu^-$  naturally came out through the gauged covariant derivative approach. Nevertheless, from the EFT point of view, the matter likely springs from the missing piece of the neutral gauge boson.

The other way to cancel the divergence in the extra arbitrary magnetic moment interaction term by the  $\zeta$ -limiting ( $\zeta \rightarrow 0$ ) formalism is a technical aspect of the field theory discussed by T. D. Lee and C. N. Yang [10], which introduced a negative metric deemed as ghost particle, spin-0 component in vector field with negative norm, provides a way to regulate the theory that would otherwise make the theory non-renormalizable.

---

<sup>1</sup>The MDM's form factor expressions are under the approximation of the heavily charged boson and expand to second order  $\mathcal{O}\left(\frac{m_i^2}{m_{V,\phi}^2}\right)$ .

We'll see that, if only one chirality is involved, the charged scalar and vector contributions display negative and positive effects, respectively, on the charged ( $Q_l < 0$ ) lepton's anomalous MDM  $a_l = \frac{2m_l F_2^{V,\phi}}{-eQ_l}$  value as the  $l_k$  is neutral, for instance in the SM context, or some beyond the SM contexts, like leptoquark or lepton number violation interaction structure. Conversely, the oppositely changed sign of effect would happen as the mediator is neutral ( $Q_{V,\phi} = 0$ ) or the positively charged fermion ( $Q_k > 1$ ) inside the loop.

The EDM form factor is achieved by switching out  $m_i \rightarrow -m_i$  and  $V_L^{*ki} (Y_L^{*ki}) \rightarrow -V_L^{*ki} (Y_L^{*ki})$ , roughly speaking

$$G_2^{\phi,V} \propto (m_j - m_i) (R^{*ki} R^{kj} - L^{*ki} L^{kj}) f_1 + m_k (R^{*ki} L^{kj} - L^{*ki} R^{kj}) f_2 \quad (4.23)$$

where  $L, R$  are the left and right couplings of the newly introduced charged boson and two form factors  $f_1, f_2$ . In  $l_i = l_j$ , the electric dipole value obtained from the EDM form factor is only proportional to  $(R^* L - L^* R)$ . Then if the initial premise, which states that the left and right coupling's relative phase is different by an integer of  $\pi$  for CP invariance (CPV-free), holds true, the EDM thus equals zero for a completely CPV-free theory.

# Chapter 5

## Coupling Constraints in muon decay experiments

In this chapter, we are going to discuss the constraints within the SM context, where no new charged fermion is introduced, and the non-Lepton Flavor Violation (nLFV) of the coupling scenario equivalent to flavor diagonal coupling is assumed. We also go about investigating two universality and non-universality cases, which eventually lead to some interesting conclusions. In the last section, we will apply the EFT calculation framework to simple coupling patterns inspired by UV models.

### 5.1 Case of universal coupling

In this numerical analysis, we assumed the universal coupling within flavor-conserved and SM particle conditions. The input parameters used are:

- $\rho = 0.74979(26)$
- $\delta = 0.75047(34)$
- $|\xi| = 1.0009^{+0.0016}_{-0.0007}$
- $G_F^\mu = 1.1663787(6) \times 10^{-5} \text{ GeV}^{-2}$

- $G_F^{Zl^+l^-} = 1.1661(16) \times 10^{-5} \text{ GeV}^{-2}$
- $G_F^Z = 1.1668(11) \times 10^{-5} \text{ GeV}^{-2}$

Considerably saying, according to Eq. 3.4, the  $\delta$  in this scenario should be identical to SM's predicted value of  $3/4$ , leading the universality coupling assumption to be invalid within the  $1\sigma$  uncertainty regime of Michel parameters. Thus, we hereafter extended the Michel parameters scan to  $2\sigma$  and used  $G_F^{Zl^+l^-}$  extracted from  $\Gamma_{l^+l^-}^Z = 83.984(86) \text{ MeV}$  [3, 11] and  $G_F^Z$  extracted from  $\Gamma_Z = 2.4952(23) \text{ GeV}$  as SM inputs, then attain the plot of the scanned allowable parameter space below.

- For new scalar

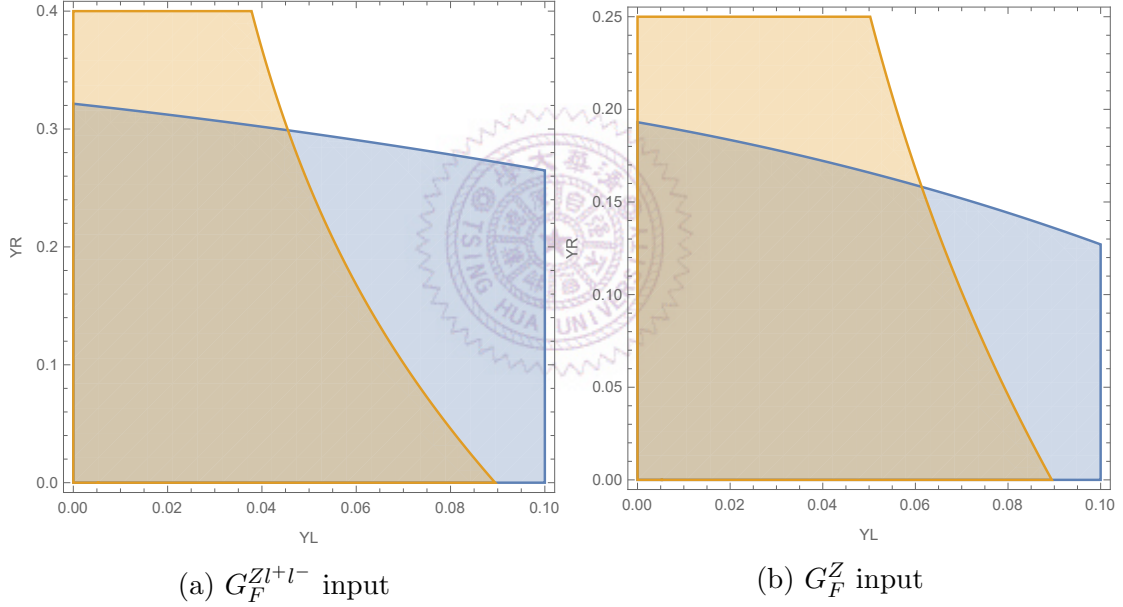


Figure 5.1: Yukawa coupling  $Y$  satisfies muon decay experiment constraints, we defined  $YL \equiv \frac{|Y^L|^2/m_\phi^2}{G_F}$ ,  $YR \equiv \frac{|Y^R|^2/m_\phi^2}{G_F}$ . The blue is represented by  $G_F$  and the orange one is represented by  $|\xi|$  constraints.

- For new vector

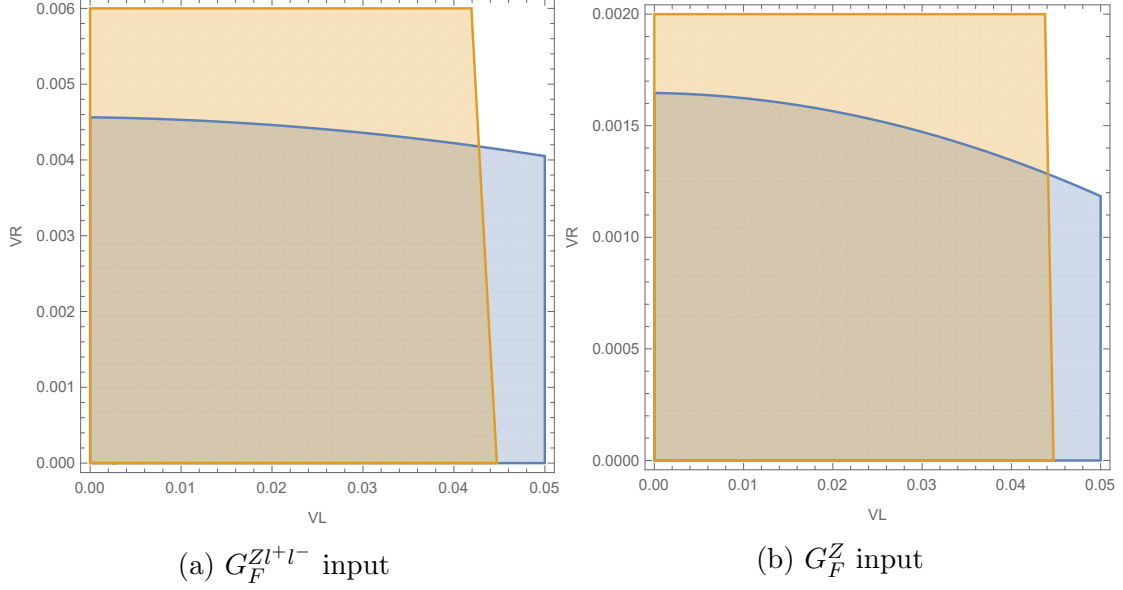


Figure 5.2: Vector coupling  $V$  satisfies muon decay experiment constraints, we defined  $VL \equiv \frac{|V^L|^2/m_V^2}{G_F}$ ,  $VR \equiv \frac{|V^R|^2/m_V^2}{G_F}$ . The blue is represented by  $G_F$  and the orange one is represented by  $|\xi|$  constraints.

Because the parameter  $\rho$  takes no significant constraint stacking up ill against the others, we have not plotted it out. The shaded area allows couplings to survive in the new scalar and vector cases depicted in Fig. 5.1-5.2, respectively, that is mainly rounded by  $|\xi|$  and  $G_F$  experiments. The bounded orange region is from  $|\xi| = 0.9995$  constraint deviating  $2\sigma$  from the mean values, whereas the bounded blue region corresponds to  $G_F^{Zl^+l^-} = 1.1645 \times 10^{-5}$  or  $G_F^Z = 1.1657 \times 10^{-5} \text{ GeV}^{-2}$  at  $1\sigma$  deviation. The  $G_F^Z$  bound from total Z decay demonstrated a stringent compass, henceforth, we are going to use it for studying later. Measuring up to  $\delta$  and  $\rho$  parameters more efficiently, the  $\xi$  parameter thus appears to be another quantity sensitive to NP, besides  $G_F$  already investigated in most literature.

## 5.2 $a_l$ contributions from new charged bosons

To simplify BSM anomalies and preserve SM symmetries, including accidental symmetries, the  $Q_{V,\phi} = 1$  charged boson is the only candidate considered. Making use of the form factor Eq. 4.1 got calculated from Eq. (4.22,4.21) in which we

derive the lepton's anomalous magnetic dipole

$$a_l = \frac{2m_l F_2^{V,\phi}}{e}. \quad (5.1)$$

- The contribution from the scalar field is apparently a negative effect

$$F_2^\phi = \frac{|Y^L|^2 + |Y^R|^2}{16\pi^2} \frac{m_l^4 - 2m_l^2 m_\phi^2 + (-2m_l^2 m_\phi^2 + 2m_\phi^4) \text{Log}\left(\frac{m_\phi^2}{m_\phi^2 - m_l^2}\right)}{2m_l^4} \quad (5.2)$$

$$= -m_l^2 \frac{|Y^L|^2 + |Y^R|^2}{96\pi^2 m_\phi^2} + \mathcal{O}\left(\frac{m_l^3}{m_\phi^3}\right) \quad (5.3)$$

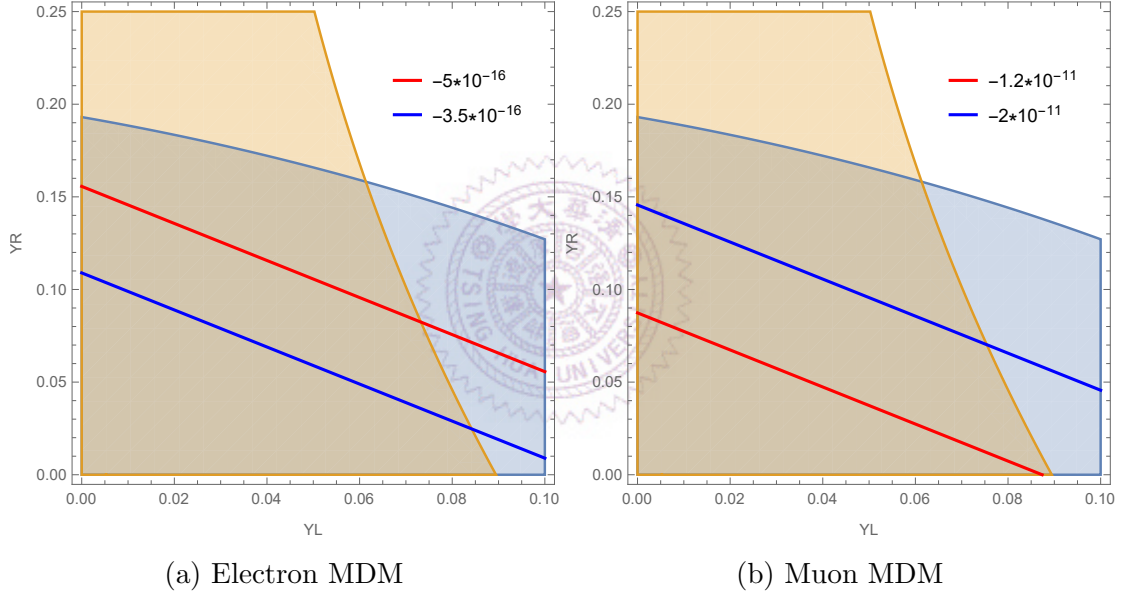


Figure 5.3: Muon MDM values from new scalar's contribution in muon decay experiment's constrained region.

- Meanwhile, the contribution from the vector field is positive

$$F_2^V = \frac{|V^L|^2 + |V^R|^2}{16\pi^2} \frac{m_l^6 + 8m_l^4 m_V^2 - 4m_l^2 m_V^4 + 2(3m_l^4 m_V^2 - 5m_l^2 m_V^4 + 2m_V^6) \text{Log}\left(\frac{m_V^2}{m_V^2 - m_l^2}\right)}{2m_l^4 m_V^2} \quad (5.4)$$

$$= 5m_l^2 \frac{|V^L|^2 + |V^R|^2}{48\pi^2 m_V^2} + \mathcal{O}\left(\frac{m_l^3}{m_V^3}\right) \quad (5.5)$$

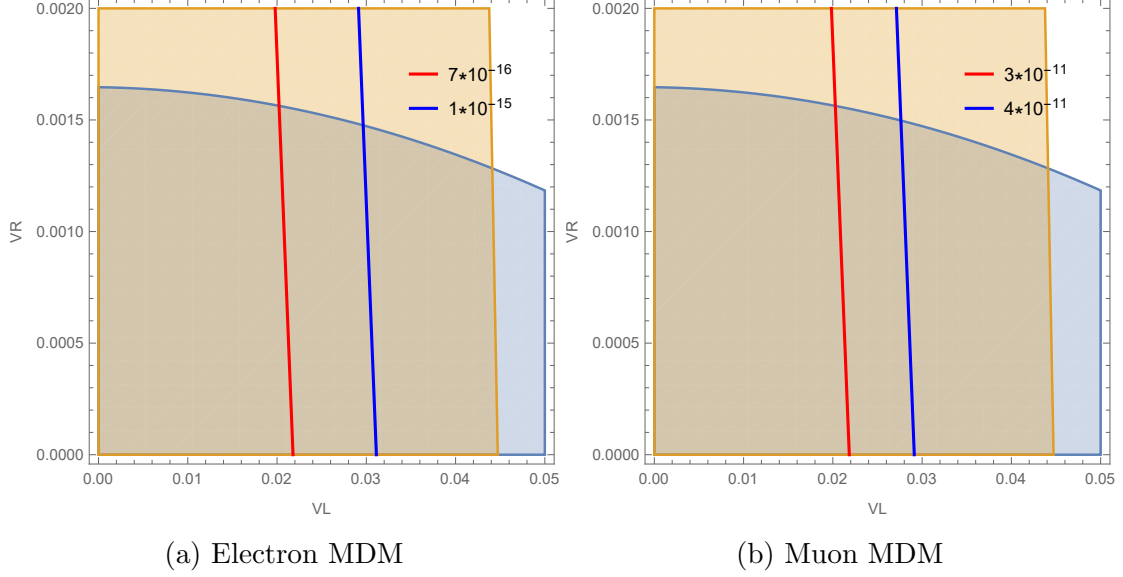


Figure 5.4: Muon MDM values from new vector's contribution in muon decay experiment's constrained region.

We can see that the MDM in the scalar case is highly constrained by the Fermi constant extracted from total Z decay, meanwhile, in the vector case, the MDM is inclined to be strongly constrained by the Michel parameter  $\xi$ . The allowed region generates merely a smidgen of MDM values, which is not enough to explain the anomaly

$$\Delta a_\mu = (2.74 \pm 0.73) \times 10^{-9} [5] \quad (5.6)$$

$$\Delta a_e = (-88 \pm 36) \times 10^{-14} [12]. \quad (5.7)$$

Frequently, in most research works, where people involved more than just only one charged boson as our simple consideration. Furthermore, the chiral enhancement happens, for example, as described in Eq. 6.49, the neutral scalar is capable of putting forward a solution for the opposite sign effect between muon and electron MDM on that account [13]. Notice that the scalar takes the negative contribution, whilst in contrast, the vector takes the positive contribution.



### 5.3 Case of non-universal coupling

In the non-universality case, we thus derived the allowed region graph for explaining the electron MDM with the new scalar, hereby, we tuned the coupling of muon to a very small value  $\frac{|Y_{\mu\nu\mu}^R|^2}{m_\phi^2} = \frac{|Y_{\mu\nu\mu}^L|^2}{m_\phi^2} = 6 \times 10^{-10}$  so as to get the safe regime in electron couplings space satisfying the electron MDM anomaly.

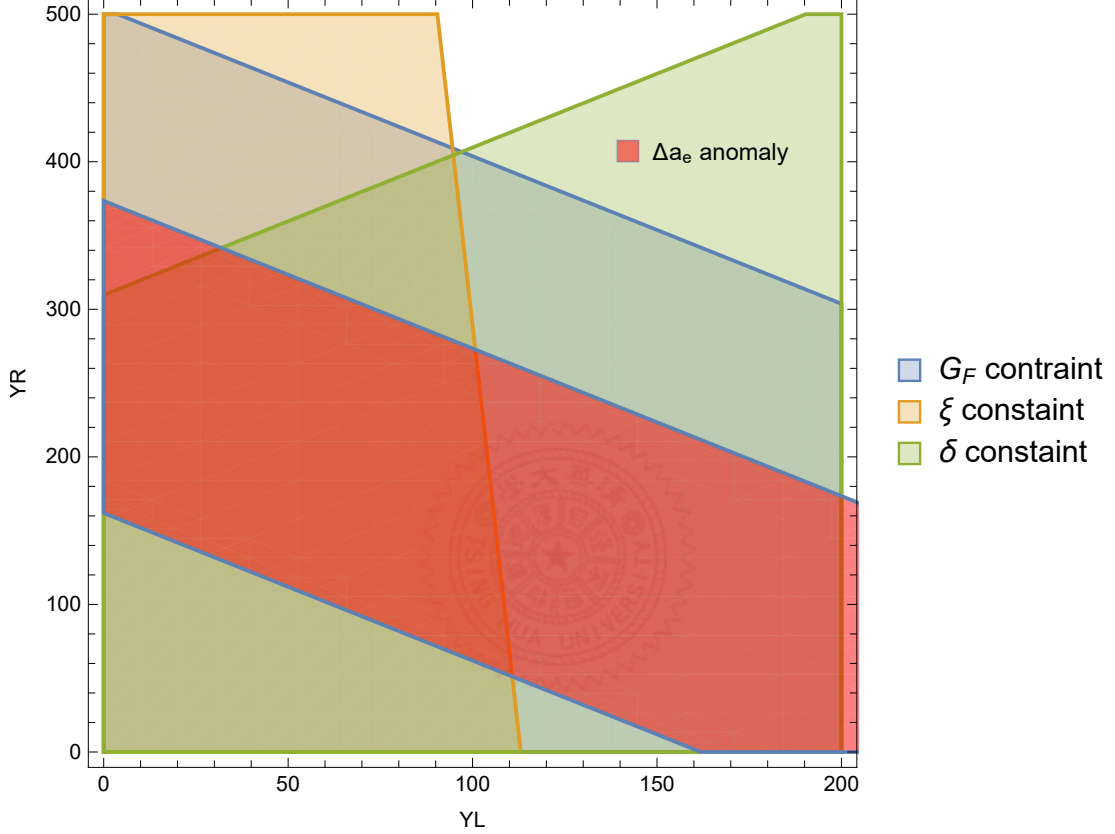


Figure 5.5: Electron MDM anomaly in the new scalar's non-universality coupling of the constrained region, we defined  $YL \equiv \frac{|Y_{e\nu e}^L|^2/m_\phi^2}{G_F}$ ,  $YR \equiv \frac{|Y_{e\nu e}^R|^2/m_\phi^2}{G_F}$ .

Now, the upper bound is no longer constrained by  $G_F$  as the universality case, it is instead from the Michel parameter  $\delta$  constraint. That emphasizes the importance of Michel parameters in probing and constraining the NP. This fine-tuning is frustrating on the theoretical side, as the coupling of the muon is smaller by two orders of magnitude of  $G_F$  the Fermi constant, while the electron's coupling is over 100 times larger than the Fermi constant. Owing to the mass hierarchy between electron and muon, speculatively saying, the theory entailing the mass inversely

associated with Yukawa coupling may help reconcile this issue, nonetheless.

Nevertheless, the complicated behavior of constraints is put up in the new vector's non-universality case, in which we chose a benchmark point in the muon coupling regime that satisfies the muon MDM anomaly and then see how the electron couplings are constrained. The same size as  $G_F$  is demanded for the vector's couplings pictured in Fig. 5.6, which is probably unreasonable given the current experimental evidences.

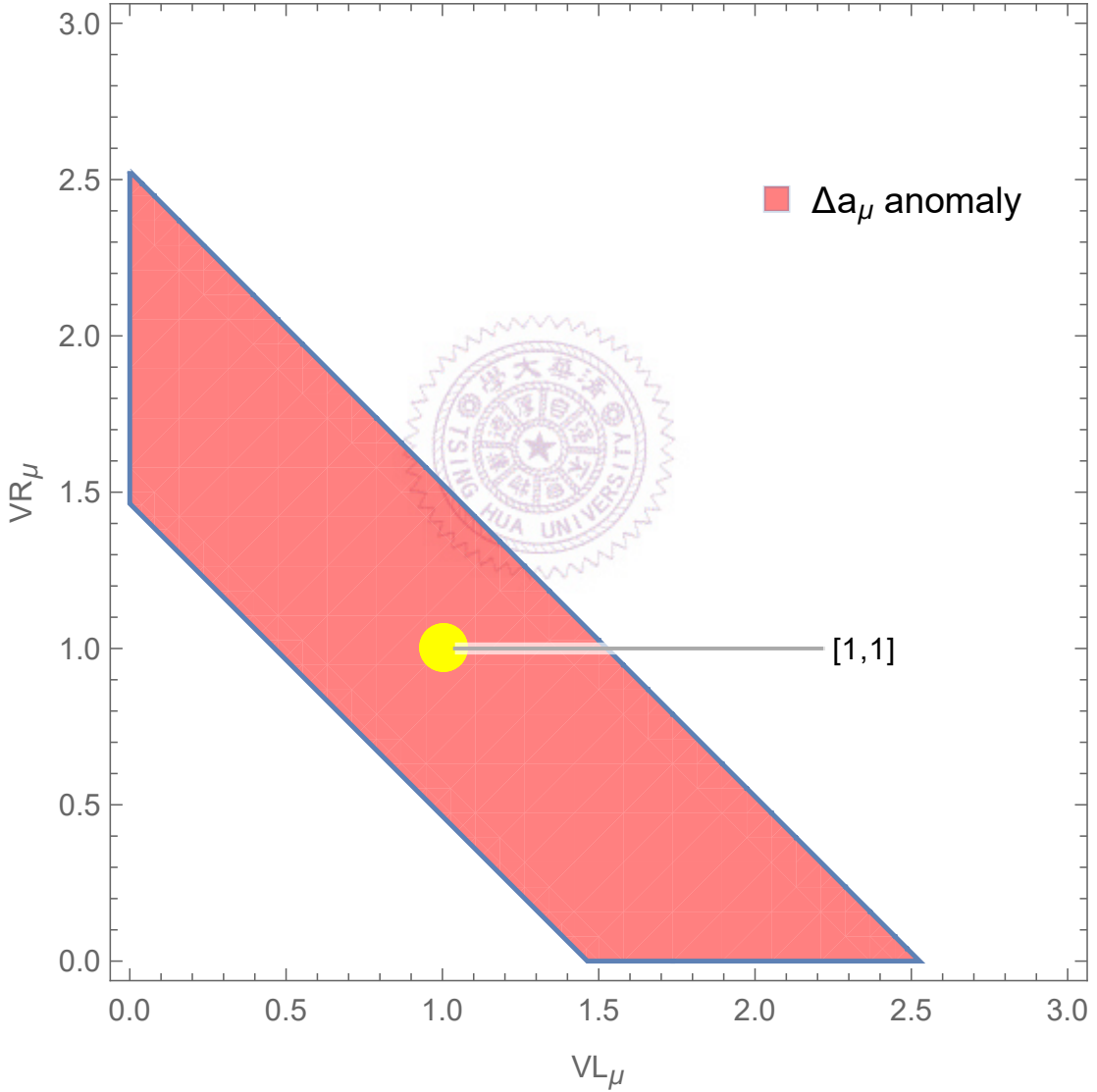


Figure 5.6: Muon MDM anomaly's allowed region in the new vector's non-universality coupling case, we defined  $VL_\mu \equiv \frac{|V_{\mu\nu\mu}^L|^2/m_V^2}{G_F}$ ,  $VR_\mu \equiv \frac{|V_{\mu\nu\mu}^R|^2/m_V^2}{G_F}$ .

Contrary to the new scalar case, the new vector has an interference effect

between the new vector and the SM  $W^\pm$  boson, which induces dependence on the relative phase between couplings. Depending on whether the interference is constructive or destructive, which is determined by the value of the relative phase, either the  $G_F$  or  $\delta$  parameter will play the dominant role in imposing constraints.

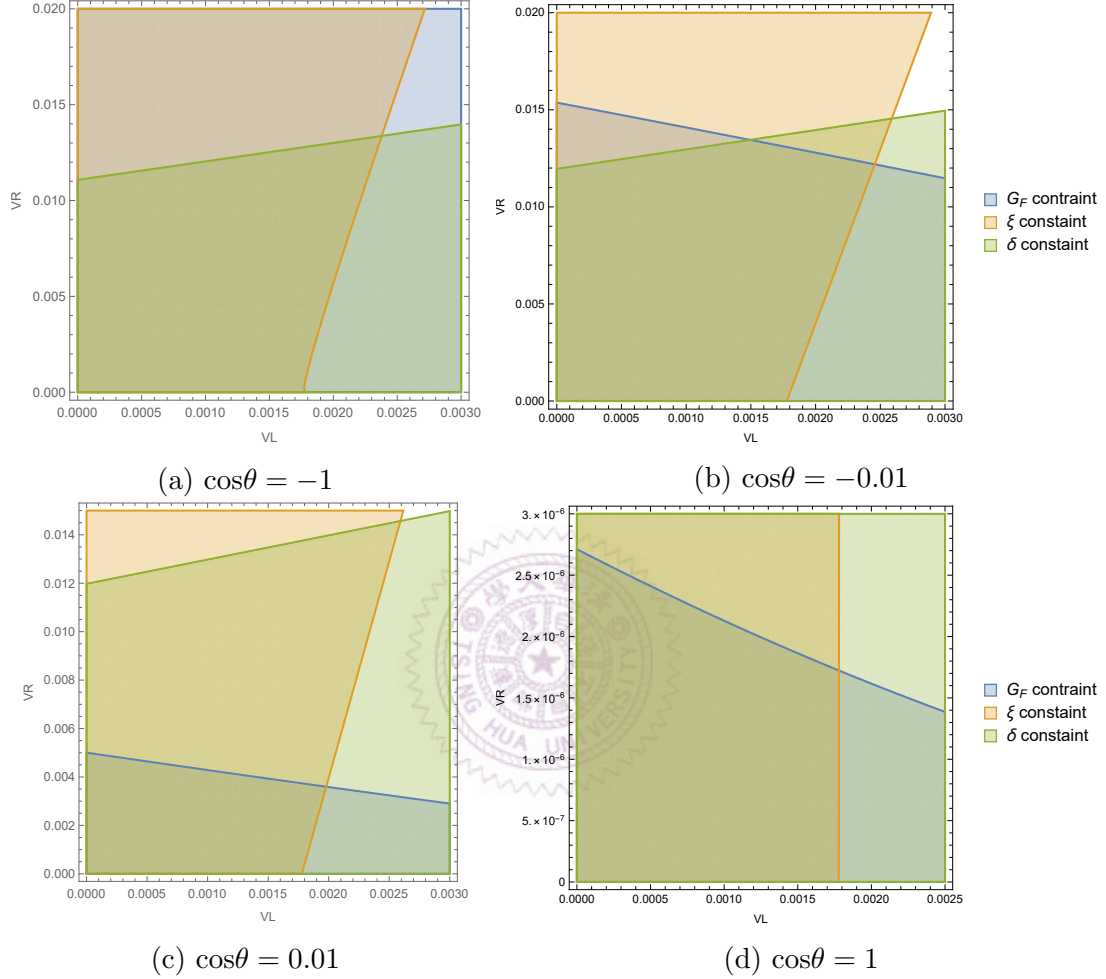


Figure 5.7: The new vector non-universality coupling's constrained region, we defined  $VL \equiv \frac{|V_{e\nu_e}^L|^2/m_V^2}{G_F}$ ,  $VR \equiv \frac{|V_{e\nu_e}^R|^2/m_V^2}{G_F}$ . The angle  $\theta$  is the relative phase between two couplings,  $V_{e\nu_e}^R$  and  $V_{\mu\nu_\mu}^{*R}$ .

As shown above in Fig. 5.7, when  $\cos\theta$  is negative, the Michel parameter  $\delta$  gives a strong constraint on the upper bound. Once  $\cos\theta$  turns positive, the  $G_F$  constraint dominates and lays down more stringent constraints in the electron coupling space.

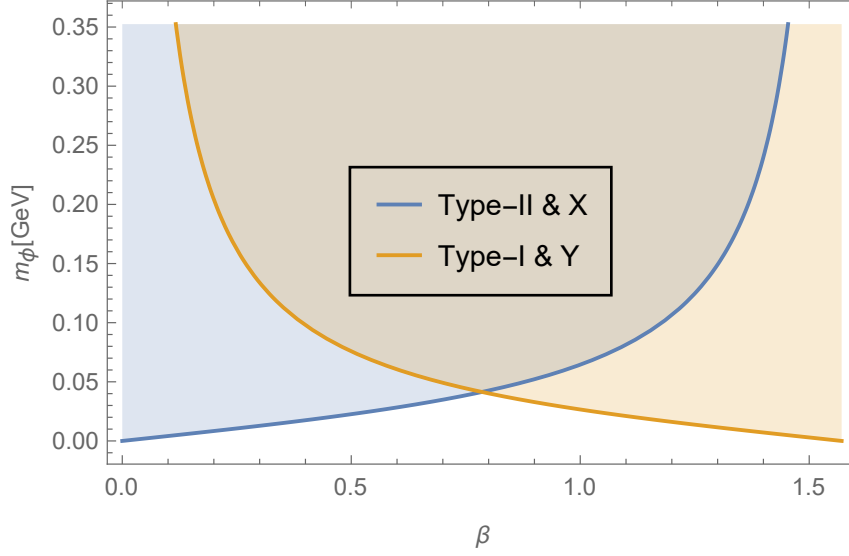


Figure 5.8: 2HDM constraint

## 5.4 Coupling pattern from UV models

In this section, we rely on the pattern from several UV models to set out limits on the mass range search for new particles. In 2HDM, the coupling conformations are summarized in table 5.1 involving only one chiral interaction

$$Y^L = -\frac{\sqrt{2}m_l\xi_l}{\langle H_{SM} \rangle}, \quad (5.8)$$

$\langle H_{SM} \rangle$  is the SM VEV mixing, characterized by  $\beta$  angle, between non-trivial vacuum expectations of two Higgs doublets

$$\langle H_{SM} \rangle = \langle H_1 \rangle \sin \beta + \langle H_2 \rangle \cos \beta. \quad (5.9)$$

Following the available procedure derived in this study, the constraint relation of mass and coupling value is shown in Fig 5.8.

Type	Description	up-type quarks couple to	down-type quarks couple to	charged leptons couple to	Coupling $\xi_l$
Type I	Fermiophobic	$H_2$	$H_2$	$H_2$	$\cot \beta$
Type II	MSSM-like <sup>1</sup>	$H_2$	$H_1$	$H_1$	$-\tan \beta$
Type X	Lepton-specific	$H_2$	$H_2$	$H_1$	$-\tan \beta$
Type Y	Flipped	$H_2$	$H_1$	$H_2$	$\cot \beta$

Table 5.1: 2HDM type of couplings

On the other hand, the searching mass limit for a heavy  $W'$  gauge boson other than SM's  $W$  boson can be enhanced by the Muon decay experiment. If considering sequential Standard Model (SSM) models, where the new extended gauge fields share similar properties to that of the SM, couplings with either left or right-handed are SM-like coupling

$$V^R (V^L) = g/\sqrt{2}. \quad (5.10)$$

From Fig 5.2, we can readily extract the lower bound of the new gauge boson mass for SSM models. The relatively strong lower limits on the mass scale for the  $W'$  boson with only left-handed and only right-handed couplings are 3.3 TeV and 637 GeV, respectively. These limits are compared to the 2016 PDG values of 3.7 TeV for left-handed coupling and 715 GeV for right-handed coupling.

These analyses serve as a test bed and provide formulas for further study. No less pivotal, the precise measurements offered by Muon decay experiments, demonstrate that here is a promising source of NP's constraint and detection.

# Chapter 6

## Constraints on Lepton Flavor

## Violation coupling applied to

## Extended Standard model Higgs

## sector



### 6.1 Zee's model

The Zee model, a notable extension of the Standard Model, offers a compelling framework for understanding the origin of neutrino masses, a key factor in explaining the well-established neutrino oscillation data. This model addresses the limitations of the Standard Model, particularly in explaining the tiny neutrino mass, which is realized through loop correction, apart from other mechanisms such as the type-I, II, and III seesaw models. This contribution, breaking the lepton number  $L_{e,\mu,\tau}$  by two units, leads to Majorana masses for neutrinos post-electroweak symmetry breaking. It introduces new particles, including an additional Higgs doublet and a singly-charged scalar, which are not excessively heavy and thus remain

within the reach of experimental verification at colliders. These new degrees of freedom are also significant in generating observable lepton flavor violating (LFV) signals, like  $\mu \rightarrow e\gamma$  and  $\mu \rightarrow 3e$ , etc., and in potentially explaining experimental anomalies such as the anomalous MDM, baryogenesis, and recently  $W^\pm$  boson mass [14, 15]. The Zee model's approach to neutrino mass generation, through one-loop Majorana neutrino masses, not only aligns with observed LFV processes but also offers testable predictions by linking these new masses and couplings to others beyond the Standard Model observables. Being associated with the lepton mass in the loop, the model put forward an acceptable solution for the neutrino mass hierarchy other than any neutrino mass generating mechanism. The simplest extension of the Standard Model 2-HDM framework that entails the non-conserved lepton number interaction to give rise to the Majorana radiative neutrino mass. Thus, the leptonic Yukawa in Higgs basis is put down as:

$$\mathcal{L}_{Yuk} \supset -Y_{\alpha\beta}^S \bar{L}_\alpha^c i\sigma_2 L_\beta S^+ - Y_{\alpha\beta}^{H_2} \bar{L}_\alpha H_2 l_\beta^R - Y_{\alpha\beta}^{H_1} \bar{L}_\alpha H_1 l_\beta^R + \text{h.c.}, \quad (6.1)$$

$L^c$  is the charge conjugate of the left-handed doublet  $L$ . The first term corresponds to the singlet charged breaking lepton number invariance in SM, the latter corresponds to the 2-HDM part, and the relevant Higgs potential terms are

$$V(H_1, H_2, S^+) \supset \mu H_1^T i\sigma_2 H_2 S^- + \lambda_6 |H_1|^2 H_1^\dagger H_2 + \text{h.c.} \quad (6.2)$$

for CP-conserved in the Higgs sector, all quartic coupling is made to be real. Note that,  $Y^S$  is an antisymmetric matrix and can be rephased to be real, on the other hand,  $Y^{H_2}$  is generally complex, but here be considered real and leptophilic for simplicity, and the SM-like Yukawa coupling  $Y^{H_1} = \frac{M_l}{\langle H_1 \rangle}$  in Higgs basis chosen to

be diagonal without loss of generality. Briefly, the weak components

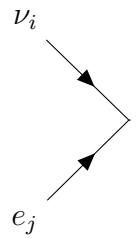
$$H_2 = \begin{pmatrix} H_2^+ \\ \frac{1}{\sqrt{2}}(H_2^0 + iA) \end{pmatrix}, \quad H_1 = \begin{pmatrix} 0 \\ \frac{H_1^0}{\sqrt{2}} \end{pmatrix}, \quad S^+ \quad (6.3)$$

are expressed by the mass eigenstates instead

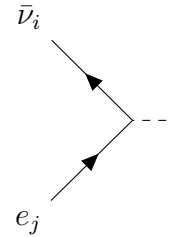
$$\begin{pmatrix} H_{SM} \\ H_N \end{pmatrix} = \begin{pmatrix} c_\alpha & s_\alpha \\ -s_\alpha & c_\alpha \end{pmatrix} \begin{pmatrix} H_1^0 \\ H_2^0 \end{pmatrix} \text{ and } \begin{pmatrix} \eta^+ \\ H^+ \end{pmatrix} = \begin{pmatrix} c_\beta & s_\beta \\ -s_\beta & c_\beta \end{pmatrix} \begin{pmatrix} S^+ \\ H_2^+ \end{pmatrix} \quad (6.4)$$

through rotation angles. Whereas the mixing in neutral scalar induced by the Higgs potential's quartic coupling  $c_\alpha s_\alpha \sim \lambda_6$  in which we consider alignment/decoupling limit ( $\alpha \rightarrow 0$ ) being compatible with LHC search [13, 16, 17],  $H_1^0 \equiv H_{SM}^1$  is then regarded as SM-like Higgs at 125 GeV and with the redefinition of  $H_0 \equiv \frac{1}{\sqrt{2}}(H_N + iA)$ . Though  $c_\beta s_\beta = \frac{\mu \langle H_1 \rangle}{m_{\eta^+}^2 - m_{H^+}^2}$  proportional to the coefficient of the cubic coupling  $\mu$  in Eq. (6.2) that breaks the lepton number by two units and contributes to non-zero Majorana neutrino mass matrix by quantum correction.

To clarify, the relevant Feynman's rules for our calculation are derived below



$$\begin{array}{c} \nu_i \\ \swarrow \\ \text{---} \nwarrow \end{array} \begin{array}{c} \eta^+ (H^+) \\ \text{---} \end{array} \quad = -ic_\beta (-s_\beta) Y_{ij}^S \hat{L} \quad (6.5)$$

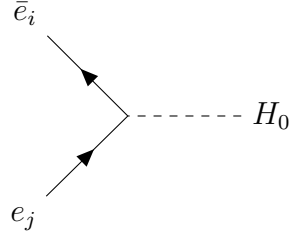


$$\begin{array}{c} \bar{\nu}_i \\ \swarrow \\ \text{---} \nwarrow \end{array} \begin{array}{c} H^+ (\eta^+) \\ \text{---} \end{array} \quad = -ic_\beta (s_\beta) Y_{ij}^{H_2} \hat{R} \quad (6.6)$$

---

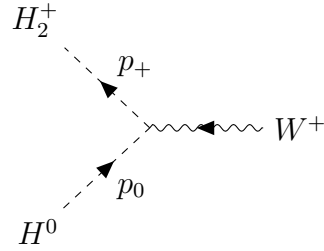
<sup>1</sup>Henceforth, which also meant  $H_2^0 \equiv H_N$ .





$$= -i \left( Y_{ij}^{H_2} \hat{R} + Y_{ji}^{H_2^*} \hat{L} \right) \quad (6.7)$$

and the final one will be employed in the next section derived from the kinematic term of doublet Higgs  $|D_\mu H_2|^2$

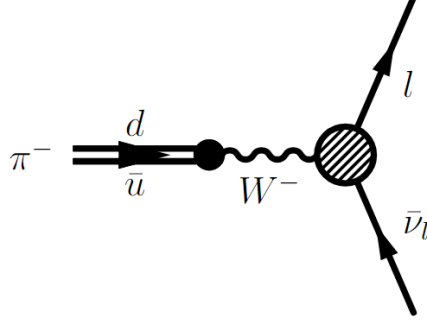


$$= -i \frac{g}{\sqrt{2}} (p_0 + p_+) \quad (6.8)$$

### 6.1.1 Universal test in Pion decay

In SM, gauge interactions are uniform across all lepton flavors, adhering to lepton flavor universality (LFU). This universality is slightly broken only by the Higgs Yukawa couplings, which are very small, around 1% for the  $\tau$  lepton. Thus, LFU is an approximate accidental symmetry of the SM at the Lagrangian level. LFU has been verified with extremely high accuracy in several systems:  $Z \rightarrow ll$  decay [ $\sim 0.1\%$ ],  $K \rightarrow (\pi)l\nu$  decay [ $\sim 0.1\%$ ],  $\tau \rightarrow l\nu\nu$  decay [ $\sim 0.1\%$ ],  $\pi \rightarrow l\nu$  decay [ $\sim 0.01\%$ ]. LFU violation (LFUV) refers to different interactions for electrons, muons, and taus leptons, distinguishable at the Lagrangian level beyond just phase-space effects. Notably, any modification to the  $W\mu\nu$  coupling, unless concurred by a change in the  $We\nu$  coupling, would affect decay rate ratios like  $R_{e/\mu}^\pi = \Gamma(\pi \rightarrow e\nu) / \Gamma(\pi \rightarrow \mu\nu)$ . Precise measurements of the ratios  $R_{e/\mu}^{\pi,K}$  and other decay channels are thus crucial for probing any SM extensions that cause nonuniversal corrections to  $Wl\nu$  couplings, see review of recent works in LUV at ref. [18].

First one of the issues that the Zee model is capable to address is the LFUV, especially pion  $\pi \rightarrow l\nu$  decay in this study. On top of that, taking a skim over how the model can play on, we calculate the newly additional effects modifying  $Wl\nu$  boson coupling.



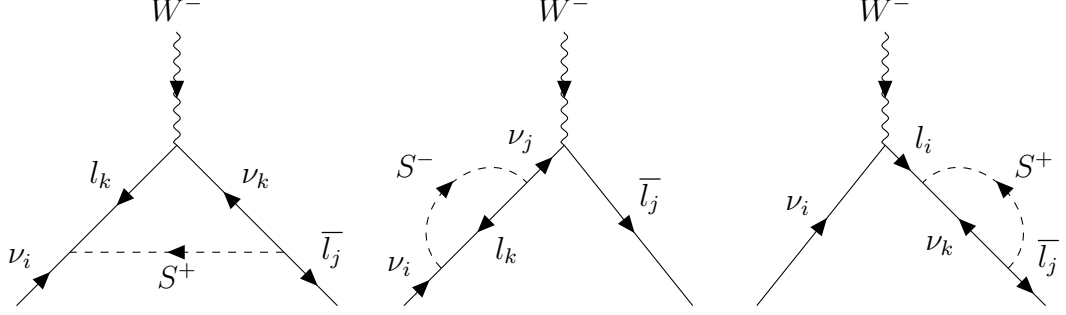
Experimental evidence, supported by theory, observed in the presence of helicity suppression <sup>2</sup>, has demonstrated the existence of a vector boson mediator and its dominant effect in pion decay. Henceforth, even though without the free-coupling to the quark sector of the second Higgs doublet is initially adopted, we are safe to ignore any tree-level interactions other than  $W^\pm$  boson. Only the first two terms in Eq. (6.1) contributes to the LFUV test at the one-loop level we must take into account

$$\begin{aligned} \mathcal{L}_{Yuk}^{Wl\nu} &\supset -Y_{\alpha\beta}^S \bar{L}_\alpha^c i\sigma_2 L_\beta S^+ - Y_{\alpha\beta}^{H_2} \bar{L}_\alpha H_2 l_\beta^R + h.c. \\ &= -Y_{\alpha\beta}^S (\bar{\nu}_\alpha^c l_\beta - \bar{l}_\alpha \nu_\beta) S^+ - Y_{\alpha\beta}^{H_2} \bar{\nu}_\alpha l_\beta^R H_2^+ - Y_{\alpha\beta}^{H_2} \bar{l}_\alpha l_\beta^R H_0 + h.c., \end{aligned} \quad (6.9)$$

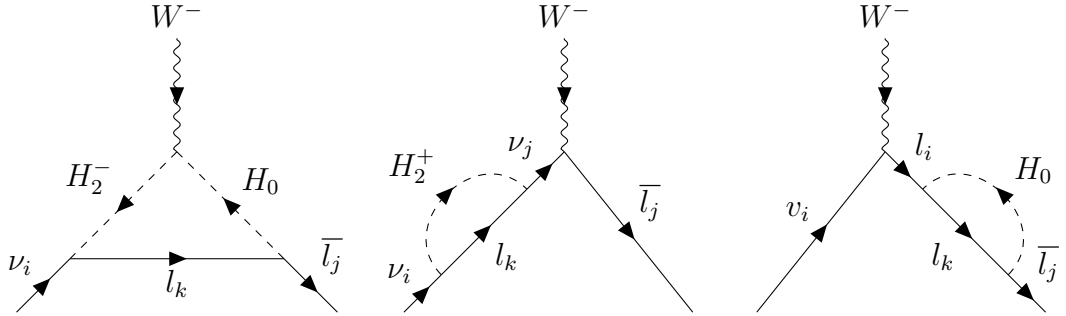
For simplicity, the neutrino and lepton masses are supposedly suppressed, except the lepton mass term presenting the helicity suppression effect. Additionally, instead of mass eigenstates, we will use the flavor state  $S^+, H_2^+, H_0$  <sup>3</sup> for this cursory calculation. The operations from the singlet are depicted below

<sup>2</sup>The helicity suppression explains the dominant decay in muons (99.99%) rather than electron.

<sup>3</sup>Definition of  $H_0 \equiv \frac{1}{\sqrt{2}} (H_2^0 + iA)$ .



Whilst, the actions from the doublet are



Note that any contribution involving lepton mass is suppressed by tiny lepton mass presumption. These six one-loop diagrams represent four loop integrals below

$$\Gamma_W^\mu = \int \frac{d^4 q}{(2\pi)^4} \frac{(\psi_i - q) \gamma^\mu (l_j + q)}{(q^2 - m_S^2) (l_j + q)^2 (\nu_i - q)^2} \quad (6.10)$$

$$\Sigma_\nu^\alpha = \int \frac{d^4 q}{(2\pi)^4} \frac{\psi_i - q}{(q^2 - m_\alpha^2) (\nu_i - q)^2} \quad (6.11)$$

$$\Sigma_l^\alpha = \int \frac{d^4 q}{(2\pi)^4} \frac{l_j + q}{(q^2 - m_\alpha^2) (l_j + q)^2} \quad (6.12)$$

$$\Gamma_W^{H_2} = \int \frac{d^4 q}{(2\pi)^4} \frac{(\nu_i + l_j) \cdot (2q + \nu_i - l_j)}{q^2 \left[ (\nu_i + q)^2 - m_{H_2^+}^2 \right] \left[ (l_j - q)^2 - m_{H_0}^2 \right]}. \quad (6.13)$$

The terms  $\Gamma_W^{H_2^4}$  and  $\Gamma_W^\mu$  denote the vertex corrections for doublets and singlets, respectively. Additionally,  $\Sigma_l^\alpha$  and  $\Sigma_\nu^\alpha$  indicate the wavefunction corrections for leptons and neutrinos, where  $\alpha \in \{S, H_2^+, H_0\}$ . Leveraging the PV-function con-

<sup>4</sup>Indeed, this is not exact correction of the  $Wl\nu$  vertex. For simplicity, we used a trick of redefinition  $\Gamma_W^{H_2} \equiv (\nu_i + l_j)_\mu (\Gamma_W^{H_2})^\mu$  instead, with the aid of pion's four momentum  $p_\mu^\pi \equiv (\nu_i + l_j)_\mu$  inserted on, then we will pull out  $p_\mu^\pi$  in the amplitude expression below. The result, therefore, is still valid within pion decay context.

vention to put them into the form

$$\Gamma_W^\mu = 2\psi_i l_j^\mu C_{12} - 2l_j l_j^\mu (C_2 + C_{22}) + 2l_j \nu_i^\mu (C_0 + C_1 + C_2 + C_{12}) \quad (6.14)$$

$$- 2\psi_i \nu_i^\mu (C_1 + C_{11}) + \gamma^\mu \psi_i l_j (C_0 + C_1 + C_2) + \gamma^\mu (B_0^\pi + m_S^2 C_0 - 2C_{00})$$

$$\Sigma_\nu^\alpha = \psi_i (B_0^\alpha + B_1^\alpha) \quad (6.15)$$

$$\Sigma_l^\alpha = l_j (B_0^\alpha + B_1^\alpha) \quad (6.16)$$

$$\Gamma_W^{H_2} = \psi_i (B_0^{H_2^+} + B_1^{H_2^+}) + l_j (B_0^{H_0} + B_1^{H_0}), \quad (6.17)$$

where the PV functions are broken down as

$$B_i^\alpha \equiv B_i^\alpha(0, m_\alpha^2, 0)$$

$$B_i^\pi \equiv B_i^\pi(m_\pi^2, 0, 0) \quad (6.18)$$

$$C_{ij\dots} \equiv C_{ij\dots}(0, 0, m_S^2, 0, 0, 0).$$

Then, the total amplitude for these diagrams are

$$M_{1-loop}^\mu = -i (Y_{ik}^S Y_{jk}^{S*} \epsilon_S + Y_{ik}^{H_2^*} Y_{jk}^{H_2} \epsilon_{H_2}) \overline{u}_{l_j} \gamma^\mu \hat{L} v_{\nu_i}, \quad (6.19)$$

with

$$\epsilon_S = \frac{1}{16\pi^2} \left[ - (B_0^S + B_1^S) + B_0^\pi - 2C_{00} + m_S^2 C_0 + m_\pi^2 (2C_0 + 2C_1 + C_2 + C_{12} - C_{22}) \right] \quad (6.20)$$

$$\epsilon_{H_2} = \frac{1}{16\pi^2} \left[ \frac{1}{2} (B_0^{H_0} + B_1^{H_0}) - \frac{1}{2} (B_0^{H_2^+} + B_1^{H_2^+}) \right] \quad (6.21)$$

is the short-hand for one-loop contributions from singlet and doublet, respectively.

A useful and traditional way to ensure that no contributions are missed is by verifying the UV convergence of the outcome. The only PV functions that exhibit

UV divergence are

$$B_0 \supset \Lambda_{UV}, \quad B_1 \supset -\frac{\Lambda_{UV}}{2}, \quad C_{00} \supset -\frac{\Lambda_{UV}}{4}, \quad (6.22)$$

with  $\Lambda_{UV}$  is regularized UV-divergent value, from which  $M_{1-loop}^\mu$  is checked the UV convergence on the fly. Consequently, the final result is wrapped up in the Fermi constant

$$\tilde{G}_F^{\pi \rightarrow ij} = G_F^{SM} (1 - Y_{ik}^S Y_{jk}^{S*} \epsilon_S - Y_{ik}^{H_2*} Y_{jk}^{H_2} \epsilon_{H_2}) \quad (6.23)$$

$$\left| \tilde{G}_F^{\pi \rightarrow ij} \right|^2 = (G_F^{SM})^2 (1 - 2 \text{Re} : Y_{ik}^S Y_{jk}^{S*} \epsilon_S + Y_{ik}^{H_2*} Y_{jk}^{H_2} \epsilon_{H_2} :) \quad (6.24)$$

The branching ratio in pion decay is therefore

$$\begin{aligned} \frac{Br(\pi \rightarrow e \nu_e)}{Br(\pi \rightarrow \mu \nu_\mu)} &= \frac{\Gamma(\pi \rightarrow e \nu_e)}{\Gamma(\pi \rightarrow \mu \nu_\mu)} = \frac{m_e^2 (m_\pi^2 - m_e^2)^2}{m_\mu^2 (m_\pi^2 - m_\mu^2)^2} \frac{\left| \tilde{G}_F^{\pi \rightarrow ee} \right|^2}{\left| \tilde{G}_F^{\pi \rightarrow \mu\mu} \right|^2} \\ &= \frac{m_e^2 (m_\pi^2 - m_e^2)^2}{m_\mu^2 (m_\pi^2 - m_\mu^2)^2} \frac{\left( 1 - 2 |Y_{ek}^S|^2 \text{Re} : \epsilon_S : - 2 |Y_{ek}^{H_2}|^2 \text{Re} : \epsilon_{H_2} : \right)}{\left( 1 - 2 |Y_{\mu k}^S|^2 \text{Re} : \epsilon_S : - 2 |Y_{\mu k}^{H_2}|^2 \text{Re} : \epsilon_{H_2} : \right)} \end{aligned} \quad (6.25)$$

and then, putting the experimental values

$$Br(\pi \rightarrow e \nu_e) = (1.23 \pm 0.004) \times 10^{-4}, \quad (6.26)$$

$$Br(\pi \rightarrow \mu \nu_\mu) = (99.9877 \pm 0.00004) \%$$

turns Eq. 6.25 into in terms of the new parameter constraint

$$\begin{aligned} &\left( |Y_{e\tau}^S|^2 - |Y_{\mu\tau}^S|^2 \right) \text{Re} : \epsilon_S : + \left( |Y_{ek}^{H_2}|^2 - |Y_{\mu k}^{H_2}|^2 \right) \text{Re} : \epsilon_{H_2} : \\ &= 0.00116 \pm 0.00162 \approx \mathcal{O}(10^{-3}). \end{aligned} \quad (6.27)$$

The analytical expression of PV functions extracted from [8, 9] helps us derive

$$\epsilon_S = \frac{1}{16\pi^2} \left[ 4 + \frac{1}{3} (1 + 2x) \pi^2 + 4 \log(-x) + (1 + 2x) \log^2 x + (2 + 4x) \text{Li}_2(1 + x) \right] \quad (6.28)$$

$$\epsilon_{H_2} = \frac{1}{32\pi^2} \log \left( \frac{m_{H_2^+}}{m_{H_0}} \right), \quad (6.29)$$

with the variable being defined as  $x = \frac{m_S^2}{m_\pi^2}$ . In the mass range  $m_S \in (100 - 1000)$  GeV and degeneracy of doublet  $m_{H_2^+} \approx m_{H_0}$ , whereby  $\text{Re} : \epsilon_S : \in \mathcal{O}(10^{-8} - 10^{-5})$ , otherwise, the  $\epsilon_{H_2} \in \mathcal{O}(1)$  takes over in the case of  $m_{H_2^+} \neq m_{H_0}$ . The final constraint is fairly weak

$$\begin{cases} \left| |Y_{e\tau}^S|^2 - |Y_{\mu\tau}^S|^2 \right| < \mathcal{O}(10^2 - 10^5) & m_S \in (100 - 1000) \text{ and } m_{H_2^+} \approx m_{H_0} \\ \left| |Y_{ek}^{H_2}|^2 - |Y_{\mu k}^{H_2}|^2 \right| < \mathcal{O}(10^{-3}) & m_{H_2^+} \neq m_{H_0} \end{cases} \quad (6.30)$$

compared to the other constraints in this study below, henceforth being out of our interest and will not be counted toward this study's parameter scan constraints. The conclusion also tells us the Zee model staying safe within the universality test in pion decay.

### 6.1.2 Neutrino Oscillation

Neutrino oscillation, a dynamic phenomenon discovered in 1998 by the Super-Kamiokande group through their analysis of atmospheric neutrinos, stands as a pivotal exploration in elementary particle physics. Over the years, advancements in experimental studies have unveiled numerous instances of neutrino oscillation across various sources, including atmospheric, solar, accelerator, and reactor neutrinos. This groundbreaking revelation challenges the traditional understanding embedded within the SM framework, proposing a new approach that necessitates

the incorporation of neutrino mass and mixing into the theoretical models. As a result, neutrino oscillation emerges as a fundamental concept, promising to propel the field of particle physics toward more comprehensive and unified theories. The basic dynamics of the interplay between neutrino and matter ones employed to probe neutrino properties is primitively written down in the charged current (CC) interaction of SM Lagrangian

$$\mathcal{L}_{\text{CC}} = -\frac{g}{\sqrt{2}}W_{\mu}^{-} \sum_{l=\{e,\mu,\tau\}} \bar{\nu}_l^L \gamma^{\mu} l^L + \text{h.c.}, \quad (6.31)$$

where the weak eigenstates  $\nu_L^l$  are presented in terms of mass eigenstates  $\nu_i^L = \sum_{l=1}^3 U_{li}^{\nu} \nu_l^L$  by an  $3 \times 3$  unitary mixing matrix  $U^{\nu}$ , the so-called Pontecorvo-Maki-Nakagawa-Sakata (PMNS) matrix which is characterized by the following standard parametrization

$$\begin{aligned} U^{\nu} &= \begin{pmatrix} 1 & 0 & 0 \\ 0 & c_{23} & s_{23} \\ 0 & -s_{23} & c_{23} \end{pmatrix} \times \begin{pmatrix} c_{13} & 0 & s_{13}e^{-i\delta_{CP}^D} \\ 0 & 1 & 0 \\ -s_{13}e^{i\delta_{CP}^D} & 0 & c_{13} \end{pmatrix} \times \begin{pmatrix} c_{12} & s_{12} & 0 \\ -s_{12} & c_{12} & 0 \\ 0 & 0 & 1 \end{pmatrix} \times \text{Diag}\left(1, e^{i\frac{\mu_1}{2}}, e^{i\frac{\mu_2}{2}}\right) \\ &= \begin{pmatrix} c_{12}c_{13} & s_{12}c_{13} & s_{13}e^{-i\delta_{CP}^D} \\ -s_{12}c_{23} - c_{12}s_{23}s_{13}e^{i\delta_{CP}^D} & c_{12}c_{23} - s_{12}s_{23}s_{13}e^{i\delta_{CP}^D} & s_{23}c_{13} \\ s_{12}s_{23} - c_{12}c_{23}s_{13}e^{i\delta_{CP}^D} & -c_{12}s_{23} - s_{12}c_{23}s_{13}e^{i\delta_{CP}^D} & c_{23}c_{13} \end{pmatrix} \times \text{Diag}\left(1, e^{i\frac{\mu_1}{2}}, e^{i\frac{\mu_2}{2}}\right) \end{aligned} \quad (6.32)$$

in terms of mixing angles  $c_{ij} (s_{ij}) \in [0, 1]$  and CP phases  $\{\mu_i, \delta_{CP}^D\} \in [0, 2\pi]$ . Therein we assumed the 3-flavor neutrino mixing  $\nu_l^L$  for  $l = \{e, \mu, \tau\}$ , which was compatible with data from invisible Z boson decay width, and three of massive neutrinos  $\{\nu_1^L, \nu_2^L, \nu_3^L\}$ . Nevertheless, the number of massive neutrinos, in general, is larger than 3, that is recently hinted at by experiments implying the possibility of the presence of light sterile neutrinos mixing with the flavor neutrinos [?].

The complex phase's d.o.f of the PMNS matrix counted as

$$\# \text{Phase d.o.f} = \begin{cases} \frac{n(n+1)}{2} - (2n - 1) = \frac{(n-1)(n-2)}{2} & \text{Dirac neutrinos} \\ \frac{n(n+1)}{2} - n = \frac{n(n-1)}{2} & \text{Majorana neutrinos} \end{cases} \quad (6.33)$$

is similar to the CKM matrix of the quark sector in the case of Dirac neutrinos. Given  $n$  flavor generation, the factor  $-1$  in the Dirac case belongs to the global phase condition. The removing  $2n - 1$  unphysical phases by field rephasing is restricted in Majorana neutrinos though, owing to only LH neutrinos involved, in that way, the neutrino fields cannot be freely rephased. As a corollary, at least 3-flavor Dirac neutrinos are required to yield 1 CP phase, in turn, only 2-flavor Majorana neutrinos are needed for 1 CP phase.

In SM formalism, the neutrino is massless, or the PMNS matrix is the identity matrix in other words. Since the neutrino oscillation firmly detected in 1998 was an obvious evidence of BSM's new physics that forced us to discriminate between the weak eigenstate and mass eigenstate of neutrino, which are generated through the interaction with the W boson and Higgs boson, respectively. The mass eigenstate is usually regarded as the “physical” state due to the invariance under Lorentz transformation, with a definite mass generated in the Yukawa sector.

The flavor notion of LH neutrinos  $\nu_l^L$  implies their reproducing mechanism, where  $\nu_l^L$  is created with  $l^L$  in CC weak process, let's say, in charged pion decay, muon and  $\beta$  decay. Experiments based on those weak processes producing neutrino to detect neutrino oscillation data are categorized into atmospheric and accelerator (probing  $\nu_\mu$  and  $\bar{\nu}_\mu$ ), solar ( $\nu_e$ ) and reactor ( $\bar{\nu}_e$ ). The extracting experimental values of mixing angle and mass squared difference in accordance with the experiments are thus coined respectively. For instance, the neutrino solar mixing angle and mass squared differences are now and then named for  $c_{12} \equiv c_\odot$



and  $\Delta m_{21}^2 \equiv \Delta m_{\odot}^2$ , and the neutrino atmospheric referring to as  $c_{23} \equiv c_A$  and  $\Delta m_{31}^2 \equiv \Delta m_A^2$  correspondingly. Due to the smallness of (1,3) mixing, both solar and atmospheric neutrino oscillations are approximately the 2-flavor oscillation. Note that, most neutrino oscillation experiments are of the disappearance type measuring “ $\nu$  survival probability”<sup>5</sup> as they travel from the experiment source till passing the neutrino detector, they apparently cannot be used to search for CP violation. Moreover, these normal lepton-number-conserving neutrino oscillations depend only upon the Dirac phase detected through the rephasing invariant  $J_{CP}$

$$J_{CP} = \frac{\text{Im} (U_{in}^\nu U_{jm}^\nu U_{im}^{\nu*} U_{jn}^{\nu*})}{\sum_k \epsilon_{ijk} \sum_l \epsilon_{nml}} = c_{12} c_{13}^2 c_{23} s_{12} s_{13} s_{23} \sin (\delta_{CP}^D), \quad (6.34)$$

which is known as the Jarlskog invariant [19]. Hence, such oscillation experiments cannot tell us whether neutrinos are Dirac or Majorana particles.

Theoretical speaking, Dirac or Majorana neutrino refers to its mass term

$$\mathcal{L}_{M_\nu} = -M_D^{ij} \overline{\nu_i^R} \nu_j^L - \frac{1}{2} M_M^{ij} \overline{\nu_i^L} (\nu_j^L)^c + h.c., \quad (6.35)$$

with the first term called the well-known Dirac mass term and the specially second term called Majorana mass. In contrast to Dirac fermions associated with Dirac mass, Majorana fermions involve only left or right-handed field to form a “physical” state  $\Psi_\nu \equiv (\nu^L)^c + \nu^L$ , which is the solution of Dirac equation of motion, whereby being identical to its antiparticle  $\Psi_\nu = \Psi_\nu^c$  as a physical phenomenology. In general, those two kinds of mass terms are able to exist in the Lagrangian, a well-known instance is the type-I see-saw mechanism. While the  $(\nu^L)^c$  acts like  $\nu^R$  under Lorentz transformation, the Dirac mass term entails an extra new right-handed neutrino, often called sterile neutrino, being inert with SM interactions. It stands

---

<sup>5</sup>Survial probability means the probability a type of flavor neutrino is still in the same flavor as the source when it reaches the detector, e.g.  $\text{Pr}(\nu_e \rightarrow \nu_e)$ .

to reason why we got the normalized factor  $\frac{1}{2}$  in the Majorana mass term owing to half d.o.f compared to the Dirac case. The usual practical and most sensitive way to tell apart neutrino nature is through the Neutrinoless double beta decay  $0\nu\beta\beta$  decay, where an atom  $(A, Z) \rightarrow (A, Z + 2) + e^- + e^-$  decays violating the lepton number conservation.

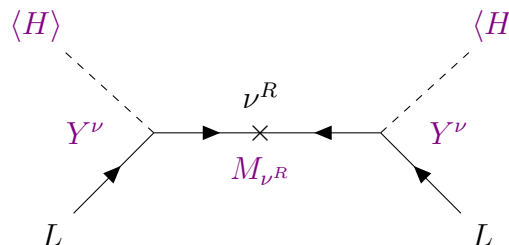
The Dirac mass term is ordinarily reproduced through the SSB mechanism from the Yukawa interaction, while the Majorana mass term is non-trivial that demands the BSM operations. At minimal extension, to form a singlet creating the neutrino's mass from doublet lepton  $L$  and/or scalar  $H$ , we have theoretically several choices. Since  $L$  and  $H$  are SU(2) doublets

$$2 \otimes 2 = 1 \oplus 3, \quad (6.36)$$

the new field thus must be either SU(2) singlet or triplet, but not a doublet. Whereby, there are the following options:

1. **New fermion field with Hypercharge  $Y = 0$**

$\oplus$  Singlet fermion  $\nu^R$ :  $Y_{ij}^\nu \bar{\nu}_i^R \tilde{H}^\dagger L_j$  (e.g. Type-I Seesaw sterile neutrino)



$$M_\nu = Y^\nu \frac{1}{M_{\nu^R}} (Y^\nu)^T \langle H \rangle^2$$

$\oplus$  Triplet fermion  $F$ :  $Y_{ij}^F \tilde{H}^\dagger \bar{F}_i L_j$  (e.g. Type-III Seesaw)

$$M_\nu = Y^F \frac{1}{M_F} (Y^F)^T \langle H \rangle^2$$

## 2. New scalar field with Hypercharge $Y = 2$

⊕ Scalar triplet  $\Delta$ :  $Y_{ij}^\Delta \bar{L}_i^c i \sigma_2 \Delta L_j$  (e.g. Type-II Seesaw)

$$M_\nu = Y^\Delta \frac{\mu_\Delta}{M_\Delta^2} \langle H \rangle^2$$

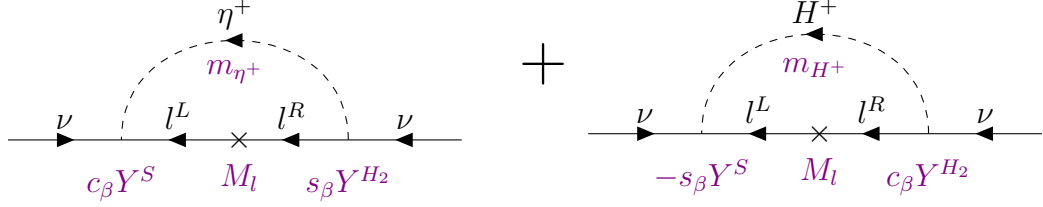
⊕ Scalar singlet  $S^+$ :  $Y_{ij}^S \bar{L}_i^c i \sigma_2 L_j S^+$  (e.g. Zee-singlet scalar)

This scenario is our case study that is elaborated on in the details and plays an important constraint in parameter scanning for our study.

The Zee model offers a non-trivial mechanism to generate a tiny radiative neutrino mass by quantum loop effects mediated by the newly heavy charged scalars. Particularly in one-loop order, we derived

$$M_\nu = \frac{\mu \langle H_1 \rangle}{16\pi^2} C_0(m_\nu^2, m_\nu^2, m_l^2, m_{\eta^+}^2, m_{H^+}^2) \left[ Y^S M_l (Y^{H_2})^T + Y^{H_2} M_l (Y^S)^T \right], \quad (6.40)$$

or equivalently, after mass diagonalization



$$M_\nu = \frac{s_\beta c_\beta}{8\pi^2} \left[ B_0(m_\nu^2, m_l^2, m_{\eta^+}^2) - B_0(m_\nu^2, m_l^2, m_{H^+}^2) \right] \left[ Y^S M_l (Y^{H_2})^T + Y^{H_2} M_l (Y^S)^T \right]. \quad (6.41)$$

In the limit  $m_{H^+}, m_{\eta^+} \gg m_l (\in M_l) \gg m_\nu (\in M_\nu)$ , the results is boiled down to concise formula

$$M_\nu = \frac{s_\beta c_\beta}{8\pi^2} \log \left( \frac{m_{\eta^+}^2}{m_{H^+}^2} \right) \left[ Y^S M_l (Y^{H_2})^T + Y^{H_2} M_l (Y^S)^T \right]. \quad (6.42)$$

According to the order estimation of mixing mass matrix, the order of Yukawa coupling is  $|Y^{S,H_2}| \sim \frac{\mathcal{O}(10^{-3}-10^{-4})}{\sqrt{|c_\beta s_\beta|}}$  in the dominant heavier scalar, and  $|Y^{S,H_2}| \sim \sqrt{\frac{m_{H^+}}{\epsilon}} \frac{\mathcal{O}(10^{-3}-10^{-4})}{\sqrt{|c_\beta s_\beta|}}$  in the nearly mass degeneracy case  $\Delta m \equiv m_{H^+} - m_{\eta^+} = \epsilon$ .

### 6.1.3 Trilepton decay constraint

The only contribution to LFV trilepton decay  $l_i \rightarrow l_j \bar{l}_m l_n$  comes from the new neutral  $H_0$  scalar, which we can traverse all  $Y^{H_2}$  coupling constraints

$$\rightarrow \Gamma(l_i \rightarrow l_j \bar{l}_m l_n) = \frac{m_i^5 \mathbf{Y}}{n! 3.2^9 \pi^3}. \quad (6.43)$$

The decay rate is derived in the approximation  $m_j, m_n, m_m \ll m_i$ , which we can ignore the final state masses, and the factor  $\mathbf{Y}$  holds in the information of Yukawa coupling of the second Higgs doublet

$$\mathbf{Y} = \frac{1}{16m_{H_0}^4} \left( |2Y_{ji}^{H_2}Y_{nm}^{H_2*} - Y_{mi}^{H_2}Y_{nj}^{H_2*}|^2 + |2Y_{ij}^{H_2}Y_{mn}^{H_2*} - Y_{im}^{H_2}Y_{jn}^{H_2*}|^2 + 4|Y_{ji}^{H_2}Y_{mn}^{H_2}|^2 \right. \\ \left. + 4|Y_{ij}^{H_2}Y_{nm}^{H_2}|^2 + 3|Y_{mi}^{H_2}Y_{nj}^{H_2}|^2 + 3|Y_{im}^{H_2}Y_{jn}^{H_2}|^2 + 4|Y_{mi}^{H_2}Y_{jn}^{H_2}|^2 + 4|Y_{im}^{H_2}Y_{nj}^{H_2}|^2 \right). \quad (6.44)$$

Employing the branching ratio

$$Br(l_i \rightarrow l_j \bar{l}_m l_n) = \frac{\mathbf{Y}}{n!128G_F^2} Br(l_i \rightarrow l_j \bar{\nu}_m \nu_n), \quad (6.45)$$

where  $G_F^i$  is the Fermi constant determined in the lepton  $l_i$  decay rate process and  $n!$  counts for undistinguished outgoing particles, we plugin the experiment data to set out the upper-bound constraint table 6.1 below

Process	Exp. data	Coupling	Constraint $\left(\frac{m_{H_0}}{\text{GeV}}\right)^4$
$\mu^- \rightarrow e^- e^+ e^-$	$< 10^{-12}$	$ Y_{ee^2}^{H_2} ^2 \left(  Y_{e\mu}^{H_2} ^2 +  Y_{\mu e}^{H_2} ^2 \right)$	$< 2.9 \times 10^{-21}$
$\tau^- \rightarrow e^- e^+ e^-$	$< 2.7 \times 10^{-8}$	$ Y_{ee^2}^{H_2} ^2 \left(  Y_{e\tau}^{H_2} ^2 +  Y_{\tau e}^{H_2} ^2 \right)$	$< 4.47 \times 10^{-16}$
$\tau^- \rightarrow \mu^- \mu^+ \mu^-$	$< 2.1 \times 10^{-8}$	$ Y_{\mu\mu}^{H_2} ^2 \left(  Y_{\tau\mu}^{H_2} ^2 +  Y_{\mu\tau}^{H_2} ^2 \right)$	$< 3.48 \times 10^{-16}$
$\tau^- \rightarrow e^- \mu^+ e^-$	$< 1.5 \times 10^{-8}$	$ Y_{\mu e}^{H_2} ^2  Y_{e\tau}^{H_2} ^2 + 2  Y_{e\mu}^{H_2} ^2  Y_{e\tau}^{H_2} ^2$ $+  Y_{e\mu}^{H_2} ^2  Y_{\tau e}^{H_2} ^2 + 2  Y_{\mu e}^{H_2} ^2  Y_{\tau e}^{H_2} ^2$	$< 7.45 \times 10^{-16}$
$\tau^- \rightarrow \mu^- e^+ \mu^-$	$< 1.7 \times 10^{-8}$	$ Y_{e\mu}^{H_2} ^2  Y_{\mu\tau}^{H_2} ^2 + 2  Y_{e\mu}^{H_2} ^2  Y_{\tau\mu}^{H_2} ^2$ $+  Y_{\mu e}^{H_2} ^2  Y_{\tau\mu}^{H_2} ^2 + 2  Y_{\mu e}^{H_2} ^2  Y_{\mu\tau}^{H_2} ^2$	$< 8.45 \times 10^{-16}$
$\tau^- \rightarrow \mu^- \mu^+ e^-$	$< 2.7 \times 10^{-8}$	$ 2Y_{\mu\tau}^{H_2} Y_{\mu e}^{H_2*} - Y_{e\tau}^{H_2} Y_{\mu\mu}^{H_2*}  + 4  Y_{\mu\tau}^{H_2} ^2  Y_{e\mu}^{H_2} ^2$ $+  2Y_{\tau\mu}^{H_2*} Y_{e\mu}^{H_2} - Y_{\tau e}^{H_2*} Y_{\mu\mu}^{H_2}  + 4  Y_{\tau\mu}^{H_2} ^2  Y_{\mu e}^{H_2} ^2$ $+ 7  Y_{e\tau}^{H_2} ^2  Y_{\mu\mu}^{H_2} ^2 + 7  Y_{\tau e}^{H_2} ^2  Y_{\mu\mu}^{H_2} ^2$	$< 2.69 \times 10^{-15}$
$\tau^- \rightarrow e^+ \mu^- e^-$	$< 1.8 \times 10^{-8}$	$ 2Y_{e\tau}^{H_2} Y_{e\mu}^{H_2*} - Y_{\mu\tau}^{H_2} Y_{ee}^{H_2*}  + 4  Y_{e\tau}^{H_2} ^2  Y_{\mu e}^{H_2} ^2$ $+  2Y_{\tau e}^{H_2*} Y_{\mu e}^{H_2} - Y_{\tau\mu}^{H_2*} Y_{ee}^{H_2}  + 4  Y_{\tau e}^{H_2} ^2  Y_{e\mu}^{H_2} ^2$ $+ 7  Y_{\mu\tau}^{H_2} ^2  Y_{ee}^{H_2} ^2 + 7  Y_{\tau\mu}^{H_2} ^2  Y_{ee}^{H_2} ^2$	$< 1.79 \times 10^{-15}$

Table 6.1: Trilepton decay constraints table

The table 6.1 can be cast into simpler expressions using the basic inequality  $a^2 + b^2 \geq 2ab$ , which is shown in table 6.2. The well-known values of the lepton decay branching ratios  $Br(\mu \rightarrow e \bar{\nu}_e \nu_\mu) \approx 100\%$  and  $Br(\tau \rightarrow l \bar{\nu}_l \nu_\tau) \approx 17.5\%$  are used here. These constraints roughly tell us the upper bound of the new doublet Higg coupling  $|Y^{H_2}| < \mathcal{O}(10^{-4}) \frac{m_{H_0}}{\text{GeV}}$ .

Process	Exp. data	Coupling	Constraint $(\frac{m_{H_0}}{GeV})^4$
$\mu^- \rightarrow e^- e^+ e^-$	$< 10^{-12}$	$ Y_{ee}^{H_2} ^2  Y_{e\mu}^{H_2}   Y_{\mu e}^{H_2} $	$< 1.45 \times 10^{-21}$
$\tau^- \rightarrow e^- e^+ e^-$	$< 2.7 \times 10^{-8}$	$ Y_{ee}^{H_2} ^2  Y_{e\tau}^{H_2}   Y_{\tau e}^{H_2} $	$< 2.24 \times 10^{-16}$
$\tau^- \rightarrow \mu^- \mu^+ \mu^-$	$< 2.1 \times 10^{-8}$	$ Y_{\mu\mu}^{H_2} ^2  Y_{\tau\mu}^{H_2}   Y_{\mu\tau}^{H_2} $	$< 1.74 \times 10^{-16}$
$\tau^- \rightarrow e^- \mu^+ e^-$	$< 1.5 \times 10^{-8}$	$ Y_{\mu e}^{H_2}   Y_{e\tau}^{H_2}   Y_{e\mu}^{H_2}   Y_{e\tau}^{H_2} $	$< 1.32 \times 10^{-16}$
$\tau^- \rightarrow \mu^- e^+ \mu^-$	$< 1.7 \times 10^{-8}$	$ Y_{e\mu}^{H_2}   Y_{\mu\tau}^{H_2}   Y_{e\mu}^{H_2}   Y_{\tau\mu}^{H_2} $	$< 1.49 \times 10^{-16}$
$\tau^- \rightarrow \mu^- \mu^+ e^-$	$< 2.7 \times 10^{-8}$	$ Y_{\mu e}^{H_2}   Y_{e\mu}^{H_2}   Y_{\tau e}^{H_2}   Y_{e\tau}^{H_2}  +  Y_{\mu\mu}^{H_2} ^2  Y_{\tau e}^{H_2}   Y_{e\tau}^{H_2} $ $-\frac{1}{8}  Y_{\mu\mu}^{H_2}  ( Y_{\mu\tau}^{H_2}   Y_{\mu e}^{H_2}   Y_{e\tau}^{H_2}  +  Y_{\tau\mu}^{H_2}   Y_{e\mu}^{H_2}   Y_{\tau e}^{H_2} )$	$< 1.68 \times 10^{-16}$
$\tau^- \rightarrow e^+ \mu^- e^-$	$< 1.8 \times 10^{-8}$	$ Y_{\mu e}^{H_2}   Y_{e\mu}^{H_2}   Y_{\tau e}^{H_2}   Y_{e\tau}^{H_2}  +  Y_{ee}^{H_2} ^2  Y_{\tau\mu}^{H_2}   Y_{\mu\tau}^{H_2} $ $-\frac{1}{8}  Y_{ee}^{H_2}  ( Y_{\mu\tau}^{H_2}   Y_{e\mu}^{H_2}   Y_{e\tau}^{H_2}  +  Y_{\tau\mu}^{H_2}   Y_{\mu e}^{H_2}   Y_{\tau e}^{H_2} )$	$< 1.11 \times 10^{-16}$

Table 6.2: Simple expression of Trilepton decay constraints

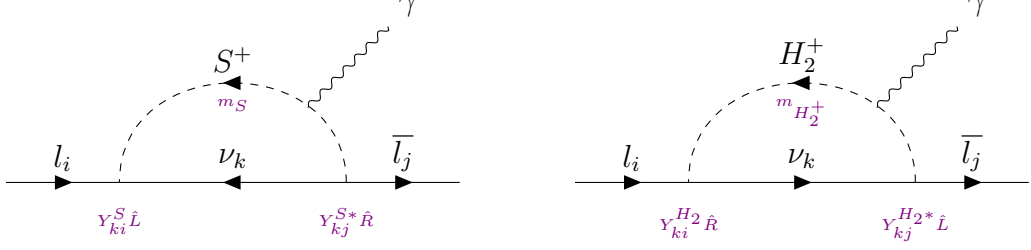
#### 6.1.4 $L \rightarrow l\gamma$

Another of the LFV decays we should count in is the well-known lep-to-lep-gamma channel. The tiny neutrino mass insertion suppresses the mixing doublet-singlet coupling term, thereby negligible

$$\sim m_\nu \frac{c_\beta s_\beta}{m_{\eta^+(H^+)}^2} Y^S Y^{H_2} \simeq 0. \quad (6.46)$$

While the main effect comes from the new neutral scalar  $H_0$

and these two sub-contributions from charged scalars



As per Eq. 4.18, to extract the branching ratio, dipole terms only needed are read off following the general formula in Eq. 4.21 <sup>6</sup>, putting down properly in

$$F_2^{H_2^+(S^+)} = \frac{-e}{3.27\pi^2} \frac{m_i + m_j}{m_{H_2^+(S)}^2} Y_{ki}^{H_2(S)} Y_{kj}^{H_2(S)*} \quad (6.47)$$

$$G_2^{H_2^+(S^+)} = \frac{e}{3.27\pi^2} \frac{m_i - m_j}{m_{H_2^+(S)}^2} Y_{ki}^{H_2(S)} Y_{kj}^{H_2(S)*} \quad (6.48)$$

for charged scalar impacts, and in effect of neutral ones otherwise

$$F_2^{H_2^0(A)} = \frac{e}{3.27\pi^2} \frac{m_i + m_j}{m_{H_2^0(A)}^2} \left[ (Y_{ki}^{H_2} Y_{kj}^{H_2*} + Y_{jk}^{H_2} Y_{ik}^{H_2*}) \right. \\ \left. \mp \frac{3m_k}{m_i + m_j} \left( 3 + 4 \log \frac{m_k}{m_{H_2^0(A)}} \right) (Y_{ki}^{H_2} Y_{jk}^{H_2} + Y_{ik}^{H_2*} Y_{kj}^{H_2*}) \right] \quad (6.49)$$

$$G_2^{H_2^0(A)} = \frac{e}{3.27\pi^2} \frac{m_i - m_j}{m_{H_2^0(A)}^2} \left[ (Y_{ki}^{H_2} Y_{kj}^{H_2*} - Y_{jk}^{H_2} Y_{ik}^{H_2*}) \right. \\ \left. \pm \frac{3m_k}{m_i - m_j} \left( 3 + 4 \log \frac{m_k}{m_{H_2^0(A)}} \right) (Y_{ki}^{H_2} Y_{jk}^{H_2} - Y_{ik}^{H_2*} Y_{kj}^{H_2*}) \right]. \quad (6.50)$$

The  $(\mp)$  sign difference in the neutral one case is induced by the CP property distinction of scalar  $H_2^0$  and pseudo scalar  $A$ , whilst  $m_S, m_{H_2^+}$  are the convention masses respective to charged singlet and doublet. The second part in Eq. (6.49-6.50) representing the chiral enhancement is canceled out in the neutral scalars degenerated case. The flavor states  $S^+, H_2^+$  adopted are possibly converted to the

---

<sup>6</sup>Recall that we initially assumed in the case of the much heavier new scalar mediators than leptons



mass eigenstates, by substituting

$$\frac{1}{m_S^2} \rightarrow \frac{c_\beta^2}{m_{\eta^+}^2} + \frac{s_\beta^2}{m_{H^+}^2} \quad (6.51)$$

$$\frac{1}{m_{H_2^+}^2} \rightarrow \frac{s_\beta^2}{m_{\eta^+}^2} + \frac{c_\beta^2}{m_{H^+}^2} \quad (6.52)$$

to get the physical result after mass diagonalization. From the experiment value

$$Br(\mu \rightarrow e\gamma) : 5.7 \times 10^{-13}, \quad Br(\tau \rightarrow e\gamma) : 3.3 \times 10^{-8}, \quad Br(\tau \rightarrow \mu\gamma) : 4.4 \times 10^{-8},$$

and the branching ratio is theoretically evaluated by following through

$$Br(l_i \rightarrow l_j \gamma) = \frac{24\pi^2}{m_i^2 G_F^2} (|F_2|^2 + |G_2|^2) Br(l_i \rightarrow l_j \nu \bar{\nu}), \quad (6.53)$$

we are able to give a ballpark estimate of  $\frac{|Y^{S,H_2}|^2}{m_{S,H_2}^2} < \mathcal{O}(10^{-8} - 10^{-6}) \text{ GeV}^{-2}$  <sup>7</sup>.

Given the mass of neutral scalars is much heavier than charged scalars, the constraint suppresses the LFV ones, see in table 6.1, on account of the dominant contribution of charged scalars. On the other hand, the neutral ones take over the space and waive off constraints from singlet coupling  $Y^S$  in the more massive charged scalars scenario, letting the Michel parameters constraint room to cook up. The table 6.3 refers to the degeneracy of neutral scalar as  $m_{H_2^0} \approx m_A \equiv m_{H_0}$ , and the coupling combinations are defined as follows

$$\frac{|Y_{ij}^{F_2}|^2}{m_{S,H_2}^2} = \left[ 2 \frac{(Y_{ki}^{H_2} Y_{kj}^{H_2*} + Y_{jk}^{H_2} Y_{ik}^{H_2*})}{m_{H_0}^2} - \sum_{\alpha=S^+, H_2^+} \frac{Y_{ki}^\alpha Y_{kj}^{\alpha*}}{m_\alpha^2} \right] \quad (6.54)$$

$$\frac{|Y_{ij}^{G_2}|^2}{m_{S,H_2}^2} = \left[ 2 \frac{(Y_{ki}^{H_2} Y_{kj}^{H_2*} - Y_{jk}^{H_2} Y_{ik}^{H_2*})}{m_{H_0}^2} + \sum_{\alpha=S^+, H_2^+} \frac{Y_{ki}^\alpha Y_{kj}^{\alpha*}}{m_\alpha^2} \right]. \quad (6.55)$$

---

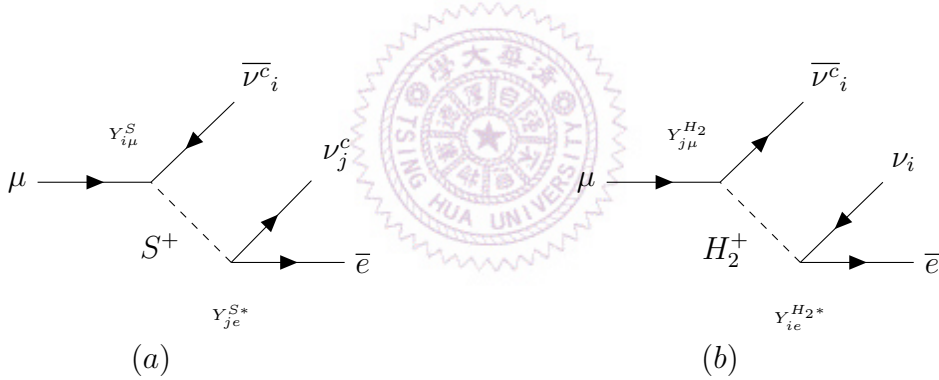
<sup>7</sup>The notation  $m_{S,H_2}^2$  stands for a set of  $\{m_{\eta^+}^2, m_{H^+}^2, m_{H_2^0}^2, m_A^2\}$

Process	Exp. data	Coupling	Constraint
$\mu^- \rightarrow e^- \gamma$	$< 5.7 \times 10^{-13}$	$\frac{ Y_{\mu e}^{G_2} ^4}{m_{S,H_2}^4} + \frac{ Y_{\mu e}^{F_2} ^4}{m_{S,H_2}^4}$	$< 2.93 \times 10^{-16}$
$\tau^- \rightarrow e^- \gamma$	$< 3.3 \times 10^{-8}$	$\frac{ Y_{\tau e}^{G_2} ^4}{m_{S,H_2}^4} + \frac{ Y_{\tau e}^{F_2} ^4}{m_{S,H_2}^4}$	$< 1.70 \times 10^{-11}$
$\tau^- \rightarrow \mu^- \gamma$	$< 4.4 \times 10^{-8}$	$\frac{ Y_{\tau \mu}^{G_2} ^4}{m_{S,H_2}^4} + \frac{ Y_{\tau \mu}^{F_2} ^4}{m_{S,H_2}^4}$	$< 2.26 \times 10^{-11}$

Table 6.3: Lep-to-lep-gamma constraints table

### 6.1.5 Muon decay

In the compass of this study, the additional come-up of the singlet scalar strikes up in muon decay, which gets contributions of doublet charged Higgs either. The Feynman diagrams scale up from 2 to 8 after mass diagonalization, inducing the singlet-doublet mixing terms. The first two contributions are from singlet and doublet, respectively



The two Michel parameters keep intact  $\rho = \delta = \frac{3}{4}$  compared to SM prediction despite these two unmixed effects from singlet and doublet charged scalar above get into, which is due to their non-sensitivity to the chirality distinction. Meanwhile, the  $\xi$  parameter is able to achieve the new physics effect through  $b(b')$  parameter as defined in Eq (??)

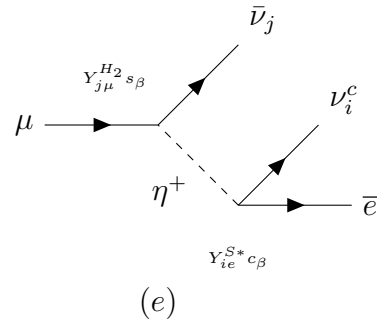
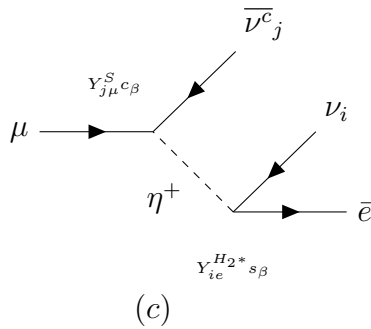
$$b(b') = \left( \sqrt{2}G_F^{SM} + \frac{|Y_{e\mu}^S|^2}{4m_S^2} \right)^2 + \frac{1}{16m_S^4} \sum_{i,j \neq \{e,\mu\}} |Y_{i\mu}^S|^2 |Y_{je}^S|^2 + (-) \frac{1}{16m_{H_2^+}^4} \sum_{i,j} |Y_{i\mu}^{H_2}|^2 |Y_{je}^{H_2}|^2. \quad (6.56)$$

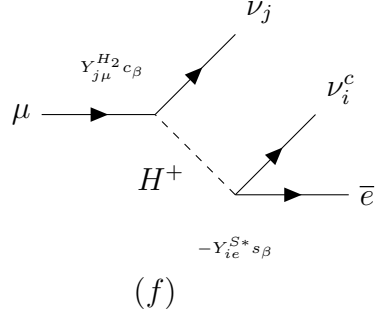
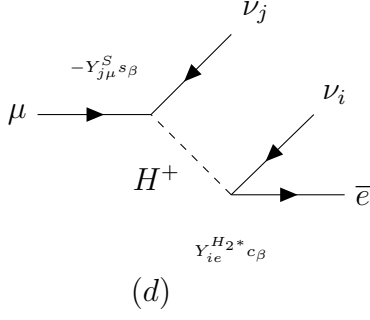
The aforementioned intrinsic difference between chiral scalar and vector-form couplings brought up the sign change of  $b$  relative to  $b'$ . Notably, as mentioned in Chapter 3, the scalar coupling from the doublet has no intertwining with respect to vector-form coupling attributed to the spin-flip difference, that produces the  $\xi$  constraint as a corollary. In contrast, the first diagram with Lepton Number Violation (LNV) Yukawa couplings puts on the vector-like form after Fierz transformation, for instance

$$\begin{aligned}
\bar{\nu}_e^c \hat{L}_\mu \bar{e} \hat{R}_\mu^c &\xrightarrow[\text{Transform}]{\text{Fierz}} -\frac{1}{4} [\bar{\nu}_\mu \gamma^\mu \nu_e \bar{e}_L \gamma_\mu \mu_L + \bar{\nu}_\mu \gamma^\mu \gamma_5 \nu_e \bar{e}_L \gamma_\mu \gamma_5 \mu_L] \\
&\xrightarrow[\text{Transform}]{\text{Fierz}} \frac{1}{2} \bar{e} \gamma^\mu \hat{L} \nu_e \bar{\nu}_\mu \gamma_\mu \hat{L} \mu,
\end{aligned} \tag{6.57}$$

therefore exhibiting a strong constructive interference with W boson, the new effect thereof just only shows up in Fermi constant constraint, where we will pick up that later.

The next four diagrams present the mixing properties between normal and LNV Yukawa couplings that open the possibility of detecting new physics in Michel parameters





These two distinct processes display the lepton number violation  $\Delta L = -2$  for the first two diagrams and  $\Delta L = 2$  for the latter two. The interference effect between singlet and doublet scalar gives rise to non-trivial contribution to decay parameters, which interestingly displays pseudo-left-right mixing effect by through the coupling combinational parameters Eq. (3.6-3.10)

$$a_{-2} = a'_{-2} = \left( \frac{1}{m_{\eta^+}^2} - \frac{1}{m_{H^+}^2} \right)^2 \frac{c_\beta^2 s_\beta^2}{16} |Y_{j\mu}^S Y_{ie}^{H2*} - Y_{i\mu}^S Y_{je}^{H2*}|^2 \quad (6.58)$$

$$c_{-2} = -c'_{-2} = \left( \frac{1}{m_{\eta^+}^2} - \frac{1}{m_{H^+}^2} \right)^2 \frac{c_\beta^2 s_\beta^2}{16} |Y_{j\mu}^S Y_{ie}^{H2*} + Y_{i\mu}^S Y_{je}^{H2*}|^2 \quad (6.59)$$

and

$$a_2 = -a'_2 = \left( \frac{1}{m_{\eta^+}^2} - \frac{1}{m_{H^+}^2} \right)^2 \frac{c_\beta^2 s_\beta^2}{16} |Y_{j\mu}^{H2} Y_{ie}^{S*} - Y_{i\mu}^{H2} Y_{je}^{S*}|^2 \quad (6.60)$$

$$c_2 = c'_2 = \left( \frac{1}{m_{\eta^+}^2} - \frac{1}{m_{H^+}^2} \right)^2 \frac{c_\beta^2 s_\beta^2}{16} |Y_{j\mu}^{H2} Y_{ie}^{S*} + Y_{i\mu}^{H2} Y_{je}^{S*}|^2 \quad (6.61)$$

corresponding to  $\Delta L = -2$ ,  $\Delta L = 2$  respectively, with no effect on  $b$ ,  $b'$  at all.

Consequently, the total contribution to parameters  $a(a') = a(a')_2 + a(a')_{-2}$  and

$c(c') = c(c')_2 + c(c')_{-2}$  alters the two Michel parameters  $\rho, \delta$  from their SM values

$$\begin{aligned}\Delta\rho &= \frac{3}{16} \left( \frac{1}{m_{\eta^+}^2} - \frac{1}{m_{H^+}^2} \right)^2 \frac{c_\beta^2 s_\beta^2}{a + 4b + 6c} \text{Re} (Y_{j\mu}^{H_2} Y_{ie}^{S*} Y_{i\mu}^{H_2*} Y_{je}^S + Y_{j\mu}^S Y_{ie}^{H_2*} Y_{i\mu}^{S*} Y_{je}^{H_2}) \\ &= (-47 - 5) \times 10^{-5}\end{aligned}\tag{6.62}$$

$$\begin{aligned}\Delta\delta &= \frac{21}{16} \left( \frac{1}{m_{\eta^+}^2} - \frac{1}{m_{H^+}^2} \right)^2 \frac{c_\beta^2 s_\beta^2}{-3a' + 4b' - 14c'} \text{Re} (Y_{j\mu}^{H_2} Y_{ie}^{S*} Y_{i\mu}^{H_2*} Y_{je}^S - Y_{j\mu}^S Y_{ie}^{H_2*} Y_{i\mu}^{S*} Y_{je}^{H_2}) \\ &= (1.3 - 8.1) \times 10^{-4}.\end{aligned}\tag{6.63}$$

Finally, all NP effects from four diagrams in muon decay add up in  $\xi$  constraint

$$\begin{aligned}|\Delta\xi| &= \frac{1}{2} \left( \frac{1}{m_{\eta^+}^2} - \frac{1}{m_{H^+}^2} \right)^2 \frac{c_\beta^2 s_\beta^2}{a + 4b + 6c} \text{Re} \left( \frac{3}{2} Y_{j\mu}^{H_2} Y_{ie}^{S*} Y_{i\mu}^{H_2*} Y_{je}^S - Y_{j\mu}^S Y_{ie}^{H_2*} Y_{i\mu}^{S*} Y_{je}^{H_2} \right) \\ &+ \frac{1}{2} \left( \frac{1}{m_{\eta^+}^2} - \frac{1}{m_{H^+}^2} \right)^2 \frac{c_\beta^2 s_\beta^2}{a + 4b + 6c} \left( |Y_{j\mu}^{H_2}|^2 |Y_{ie}^S|^2 + |Y_{i\mu}^{H_2}|^2 |Y_{je}^S|^2 \right) + \frac{1}{8m_{H_2^+}^4} \sum_{i,j} \frac{|Y_{i\mu}^{H_2}|^2 |Y_{je}^{H_2}|^2}{a + 4b + 6c} \\ &= (2 - 25) \times 10^{-4},\end{aligned}\tag{6.64}$$

and Fermi constant. As mentioned earlier, the Fermi constant is often deemed as an anomaly source of new physics contribution, in which the Zee model contributions play the new physics role, and as in the previous usage in Chapter ??, Z boson decay is benchmarked for Standard Model contribution  $G_F^{SM} \equiv G_F^Z$  compared to Fermi constant  $G_F^\mu$  precisely measured in muon decay Eq. (3.29)

$$\begin{aligned}\Delta G_F^2 &= (G_F^{\mu 2})^2 - (G_F^{SM})^2 = \frac{a + 4b + 6c}{8} - (G_F^{SM})^2 \\ &= \frac{G_F^{SM}}{2\sqrt{2}m_S^2} |Y_{e\mu}^S|^2 + \frac{1}{32m_S^4} \sum_{i,j} |Y_{i\mu}^S|^2 |Y_{je}^S|^2 \\ &+ \frac{1}{32m_{H_2^+}^4} \sum_{i,j} |Y_{i\mu}^{H_2}|^2 |Y_{je}^{H_2}|^2 + \frac{a + 6c}{8}.\end{aligned}\tag{6.65}$$

The first three terms are caused by purely singlet and doublet effects Eq. (6.56), while the last term comes from singlet-doublet mixing effect Eq. (6.58-6.61). The

likewise analytic calculation is performed for tau lepton decay, and the results are obtained by substituting the mother particle  $\mu \rightarrow \tau$  and the child particles  $\mu \rightarrow \{e, \mu\}$ . Where the decay parameter's experiment values in  $1\sigma$

$$\begin{aligned}\rho_e &= 0.747 \pm 0.010 & \rho_\mu &= 0.763 \pm 0.020 \\ \delta_e &= 0.734 \pm 0.028 & \delta_\mu &= 0.778 \pm 0.037 \\ \xi_e &= 0.994 \pm 0.040 & \xi_\mu &= 1.030 \pm 0.059\end{aligned}\tag{6.66}$$

are not strictly precise to muon decay parameters, and henceforth are out of our interest.

Roughly speaking, from the above expression of Fermi constant constraint, where  $\Delta G_F^2 \sim \mathcal{O}(10^{-13}) \text{ GeV}^{-2}$  and on the assumption  $m_{H^+} \gg m_{\eta^+}$ , the coupling strength  $\frac{|Y^{S,H_2}|^2}{m_{\eta^+}^2} < \mathcal{O}(10^{-5}) \text{ GeV}^{-2}$  cannot be too large. Along with Eq. (6.63) of the Michel parameter  $\delta$ , offhandedly  $\frac{|Y^{S,H_2}|^2}{m_{\eta^+}^2} > \frac{\mathcal{O}(10^{-7})}{|c_\beta s_\beta|} \text{ GeV}^{-2}$  evaluated, where  $-3a' + 4b' - 14c' \sim G_F^2 \sim \mathcal{O}(10^{-10}) \text{ GeV}^{-2}$  and  $c_\beta s_\beta = \frac{\mu < H_1 >}{m_{\eta^+}^2 - m_{H^+}^2}$ . Therefore, the cubic coupling  $\mu$  in Eq. (6.2) is forbidden to be arbitrarily small, and the lower bound first-step estimation is inferred

$$\mu > m_{H^+}^2 \times \mathcal{O}(10^{-4}) \text{ GeV},\tag{6.67}$$

in particular case of the much heavier one in  $\mathcal{O}(1) \text{ TeV}$  scale mass range induces  $\mu > \mathcal{O}(10^2) \text{ GeV}$ .

Michel parameters constraints impose a larger scale, say at least one order of magnitude, compared to neutrino oscillation and radiative LFV decay constraints as described by Eq. 6.42 and section 6.1.4. The very light scalar (about  $m_{\eta^+} < \mathcal{O}(100) \text{ MeV}$ ) is an easy-to-see global fitting solution that reconciles all the constraints considered so far. Nevertheless, the light charged scalar will couple to the photon, consequently being able to seek out in many experiment channels

and ruled out very well, at least below  $\mathcal{O}(10)$  GeV. Otherwise, there is no way out as Michel parameters offer a very strong constraint eliminating all feasible parameter space (based on hand-waving estimation and roughly numerical study). This conclusion is a novelty of the study. In the close mass discrepancy of two charged scalars though, we can keep the fingers crossed that there is room for the Zee model to exist. Indeed, the couplings  $|Y^{S,H_2}|^2$  in neutrino oscillation fitting are enhanced by a factor  $\frac{m_{\eta^+}}{\epsilon}$  that promisingly renders a viable solution regime, yet be aware of that the muon decay constraint is also affected by that factor, as in this case  $\frac{|Y^{S,H_2}|^2}{m_{\eta^+}^2} \sim \frac{m_{\eta^+}}{\epsilon} \frac{\mathcal{O}(10^{-7})}{|c_\beta s_\beta|} \text{ GeV}^{-2}$ .



# Chapter 7

## Conclusion and Outlook

In conclusion, this study's establishment of the low-energy EFT incorporating a novel charged boson at a low-energy scale aims to mark a significant insight into our understanding of the weak sector. The thorough verification of the anapole moment's vanishing at the one-loop order within this framework not only solidifies the theoretical footing of our approach but also assures the theoretically allowable contributions we should take into account. In addition, the extra electromagnetic interaction of the charged vector is requisite to MDM renormalized contribution, this intriguing component may hint at a novel physics originating from a neutral vector boson.

Our investigations into the lens of leptonic decays, have enabled us to place stringent constraints on the newly proposed couplings. Through analytical calculations, we were conscious of the negative and positive contribution of the new charged boson and vector respectively, potentially benefiting to tackle the electron and muon  $g - 2$  puzzle. Nevertheless, Michel parameters derived from polarized muon decay, which plays a critical role in elucidating the chirality effects embedded in the theory, through these above analyses, we have delineated a boundary for new couplings based on a  $2\sigma$  experimental uncertainty. A key finding of this research is the realization that universal coupling assumptions are insufficient to account



for the muon  $g-2$  anomaly. However, by incorporating the concept of coupling non-universality, we uncover a promising pathway to resolve this long-standing anomaly. This approach allows for a significant reduction in one lepton coupling by 2-5 magnitude order and thereby broadens the scope for other couplings. Besides that, the reason for  $2\sigma$  consideration in our Michel parameters could give us a hint on NP out of our study approach.

Furthermore, the study extends its implications to the realms of UV models, particularly in estimating the mass scale of the newly charged bosons. These predictions can surpass current experimental bounds, particularly in the LHC searches, if the Michel parameters' experiment uncertainty is strictly upgraded. Finally, in addressing the Zee Model, we have also established a strong constraint on the feasible parameter space of Yukawa couplings, and after a rough estimation, it possibly closes the door to provide the answer to the neutrino oscillation puzzle under  $1\sigma$  uncertainty of Michel parameters considered. The comprehensive and robust numerical parameter scan is being in process.

Looking forward, the framework and findings of this study offer a rich ground for theoretical development in particle physics. The theoretical advancements made here should be considered as a stepping stone towards more comprehensive models that can integrate these new bosons into the broader understanding of particle interactions. Moreover, studying the muon  $g-2$  anomaly opens up new avenues for theoretical and experimental physicists alike to explore variations in coupling strengths and their impact on other physical phenomena. Further experimental investigations will be crucial in validating the predictions made in this study and in searching for direct or indirect evidence of the new charged bosons and the unique interactions they entail.

# Chapter 8


## Appendix

### 8.1 $L \rightarrow l\gamma$ form factor

#### 8.1.1 Charged vector form factors

##### 1. Diagram a

- Dirac form factor



$$\begin{aligned}
 F_1^{V,a} = & \frac{-eQ_V}{2m_V^2} \left\{ 3 (V_{ik}^R V_{jk}^{*L} + V_{ik}^L V_{jk}^{*R}) (m_1 + m_2) m_k m_V^2 \sum_{i=0}^2 C_i^{V,a} + \right. \\
 & (V_{ik}^L V_{jk}^{*L} + V_{ik}^R V_{jk}^{*R}) \left[ \sum_{i=1}^2 \left( \frac{m_1^3 m_2^3}{m_i^2} + m_V^2 \left( 2m_1 m_2 + m_i^2 + 3 \frac{m_1^2 m_2^2}{m_i^2} \right) - m_1^2 m_2^2 \right) C_i^{V,a} - \right. \\
 & \sum_{i,j=1}^2 \left( \frac{m_1^4 m_2^4}{m_i^4} - 3 \frac{m_1^3 m_2^3}{m_i^2} - m_V^2 \left( 2m_1 m_2 + 4 \frac{m_1^2 m_2^2}{m_i^2} \right) + 2m_1^2 m_2^2 \right) C_{ij}^{V,a} - \\
 & 2 (m_1^2 + m_2^2 + 5m_1 m_2 - 6m_V^2) C_{00}^{V,a} - 6 \sum_{i=1}^2 \left( 2 \frac{m_1^2 m_2^2}{m_i^2} - 3m_1 m_2 + m_i^2 \right) C_{00i}^{V,a} - \\
 & \sum_{i,j,k=1}^2 \left( m_1^4 m_2^4 \left( \frac{1}{m_i^4} + \frac{1}{m_j^2 m_k^2} \right) - 3 \frac{m_1^3 m_2^3}{m_i^2} + m_1^2 m_2^2 \right) C_{ijk}^{V,a} - \sum_{i,j=1}^2 \left( 14 \frac{m_1^2 m_2^2}{m_i^2} - 8m_1 m_2 \right) C_{00ij}^{V,a} - \\
 & \left. \left. \sum_{i,j,k,l=1}^2 \left( 2 \frac{m_1^4 m_2^4}{m_i^2 m_j^2} - \frac{m_1^3 m_2^3}{m_i^2} \right) C_{ijkl}^{V,a} - \frac{(2m_1^2 - 7m_1 m_2 + 2m_2^2 - 6m_k^2 - 4m_V^2)^2}{4} \right] \right\}. \quad (8.1)
 \end{aligned}$$

- Anapole form factor

$$\begin{aligned}
G_1^{V,a} = & \frac{-eQ_V}{2m_V^2} \left\{ 3 (V_{ik}^R V_{jk}^{*L} - V_{ik}^L V_{jk}^{*R}) (m_1 - m_2) m_k m_V^2 \sum_{i=0}^2 C_i^{V,a} + \right. \\
& (V_{ik}^R V_{jk}^{*R} - V_{ik}^L V_{jk}^{*L}) \left[ \sum_{i=1}^2 \left( \frac{m_1^3 m_2^3}{m_i^2} + m_V^2 \left( 2m_1 m_2 - m_i^2 - 3 \frac{m_1^2 m_2^2}{m_i^2} \right) + m_1^2 m_2^2 \right) C_i^{V,a} + \right. \\
& \sum_{i,j=1}^2 \left( \frac{m_1^4 m_2^4}{m_i^4} + 3 \frac{m_1^3 m_2^3}{m_i^2} - m_V^2 \left( 4 \frac{m_1^2 m_2^2}{m_i^2} - 2m_1 m_2 \right) + 2m_1^2 m_2^2 \right) C_{ij}^{V,a} + \\
& 2 (m_1^2 + m_2^2 + 5m_1 m_2 - 6m_V^2) C_{00}^{V,a} + 6 \sum_{i=1}^2 \left( 2 \frac{m_1^2 m_2^2}{m_i^2} + 3m_1 m_2 + m_i^2 \right) C_{00i}^{V,a} + \\
& \sum_{i,j,k=1}^2 \left( m_1^4 m_2^4 \left( \frac{1}{m_i^4} + \frac{1}{m_j^2 m_k^2} \right) + 3 \frac{m_1^3 m_2^3}{m_i^2} + m_1^2 m_2^2 \right) C_{ijk}^{V,a} + \sum_{i,j=1}^2 \left( 14 \frac{m_1^2 m_2^2}{m_i^2} + 8m_1 m_2 \right) C_{00ij}^{V,a} + \\
& \left. \sum_{i,j,k,l=1}^2 \left( 2 \frac{m_1^4 m_2^4}{m_i^2 m_j^2} + \frac{m_1^3 m_2^3}{m_i^2} \right) C_{ijkl}^{V,a} + \frac{(2m_1^2 - m_1 m_2 + 2m_2^2 - 6m_k^2 - 4m_V^2)^2}{4} \right] \Bigg\}. \tag{8.2}
\end{aligned}$$

• MDM form factor

$$\begin{aligned}
F_2^{V,a} = & \frac{-eQ_V}{4m_V^2} \left\{ (V_{ik}^R V_{jk}^{*L} + V_{ik}^L V_{jk}^{*R}) m_k \left[ (m_1^2 + m_2^2 - 4m_V^2) C_0^{V,a} + \right. \right. \\
& \sum_{i=1}^2 \left( 3 \frac{m_1^2 m_2^2}{m_i^2} + m_i^2 - 6m_V^2 \right) C_i^{V,a} + 8C_{00}^{V,a} + 2 \sum_{i,j=1}^2 \frac{m_1^2 m_2^2}{m_i^2} C_{ij}^{V,a} - 1 \Bigg] - \\
& (V_{ik}^L V_{jk}^{*L} + V_{ik}^R V_{jk}^{*R}) \left[ \sum_{i=1}^2 \left( \frac{m_1^3 m_2^3}{m_i^3} - m_1 m_2 m_i + 2m_V^2 \frac{m_1 m_2}{m_i} \right) C_i^{V,a} + 8(m_1 + m_2) C_{00}^{V,a} + \right. \\
& \sum_{i,j=1}^2 \left( \frac{m_1^3 m_2^3}{m_i^3} + 2 \frac{m_1^3 m_2^3}{m_i m_j^2} - m_1 m_2 m_i + 4m_V^2 \frac{m_1 m_2}{m_i} \right) C_{ij}^{V,a} + 24 \sum_{i=1}^2 \frac{m_1 m_2}{m_i} C_{00i}^{V,a} + \\
& 4 \sum_{i,j,k=1}^2 \frac{m_1^3 m_2^3}{m_i m_j^2} C_{ijk}^{V,a} + 2 \sum_{i,j,k,l=1}^2 \frac{m_1^3 m_2^3}{m_i m_j^2} C_{ijkl}^{V,a} + 16 \sum_{i,j=1}^2 \frac{m_1 m_2}{m_i} C_{00ij}^{V,a} - \frac{7}{12} (m_1 + m_2) \Bigg] \Bigg\} -
\end{aligned}$$

$$\begin{aligned}
& \frac{aeQ_V}{4m_V^2} \left\{ (V_{ik}^L V_{jk}^{*L} + V_{ik}^R V_{jk}^{*R}) (m_1 + m_2) \left[ \sum_{i=1}^2 \left( \frac{m_1^2 m_2^2}{m_i^2} - m_1 m_2 + 2m_V^2 \right) C_i^{V,a} + 4C_{00}^{V,a} + \right. \right. \\
& \sum_{i,j=1}^2 \left( \frac{m_1^2 m_2^2}{m_i^2} - m_1 m_2 \right) C_{ij}^{V,a} \Bigg] - (V_{ik}^R V_{jk}^{*L} + V_{ik}^L V_{jk}^{*R}) m_k \left[ ((m_1 - m_2)^2 - 4m_V^2) C_0^{V,a} + \right. \\
& \left. \sum_{i=1}^2 \frac{(m_1 m_2 - m_i^2)(3m_1 m_2 - m_i^2)}{m_i^2} C_i^{V,a} + 8C_{00}^{V,a} + 2 \sum_{i,j=1}^2 \left( \frac{m_1^2 m_2^2}{m_i^2} - m_1 m_2 \right) C_{ij}^{V,a} \right] \Bigg\}. \tag{8.3}
\end{aligned}$$

• EDM form factor

$$\begin{aligned}
G_2^{V,a} = & \frac{-eQ_V}{4m_V^2} \left\{ (V_{ik}^L V_{jk}^{*R} - V_{ik}^R V_{jk}^{*L}) m_k \left[ (m_1^2 + m_2^2 - 4m_V^2) C_0^{V,a} + \right. \right. \\
& \sum_{i=1}^2 \left( 3 \frac{m_1^2 m_2^2}{m_i^2} + m_i^2 - 6m_V^2 \right) C_i^{V,a} + 8C_{00}^{V,a} + 2 \sum_{i,j=1}^2 \frac{m_1^2 m_2^2}{m_i^2} C_{ij}^{V,a} - 1 \left. \right] + \\
& (V_{ik}^L V_{jk}^{*L} - V_{ik}^R V_{jk}^{*R}) \left[ \sum_{i=1}^2 (-1)^i \left( \frac{m_1^3 m_2^3}{m_i^3} - m_1 m_2 m_i + 2m_V^2 \frac{m_1 m_2}{m_i} \right) C_i^{V,a} + 8(m_1 - m_2) C_{00}^{V,a} + \right. \\
& \sum_{i,j=1}^2 (-1)^i \left( \frac{m_1^3 m_2^3}{m_i^3} + 2 \frac{m_1^3 m_2^3}{m_i m_j^2} - m_1 m_2 m_i + 4m_V^2 \frac{m_1 m_2}{m_i} \right) C_{ij}^{V,a} + 24 \sum_{i=1}^2 (-1)^i \frac{m_1 m_2}{m_i} C_{00i}^{V,a} + \\
& 2 \sum_{i,j,k,l=1}^2 (-1)^i \frac{m_1^3 m_2^3}{m_i m_j^2} \left( C_{ijk}^{V,a} + C_{ijkl}^{V,a} \right) + 16 \sum_{i,j=1}^2 (-1)^i \frac{m_1 m_2}{m_i} C_{00ij}^{V,a} - \frac{7}{12} (m_1 - m_2) \left. \right] \left. \right\} - \\
& \frac{aeQ_V}{4m_V^2} \left\{ (V_{ik}^R V_{jk}^{*R} - V_{ik}^L V_{jk}^{*L}) (m_1 - m_2) \left[ \sum_{i=1}^2 \left( \frac{m_1^2 m_2^2}{m_i^2} + m_1 m_2 + 2m_V^2 \right) C_i^{V,a} + 4C_{00}^{V,a} + \right. \right. \\
& \sum_{i,j=1}^2 \left( \frac{m_1^2 m_2^2}{m_i^2} + m_1 m_2 \right) C_{ij}^{V,a} \left. \right] + (V_{ik}^R V_{jk}^{*L} - V_{ik}^L V_{jk}^{*R}) m_k \left[ ((m_1 + m_2)^2 - 4m_V^2) C_0^{V,a} + \right. \\
& \sum_{i=1}^2 \frac{(m_1 m_2 + m_i^2)(3m_1 m_2 + m_i^2)}{m_i^2} C_i^{V,a} + 8C_{00}^{V,a} + 2 \sum_{i,j=1}^2 \left( \frac{m_1^2 m_2^2}{m_i^2} + m_1 m_2 \right) C_{ij}^{V,a} \left. \right] \left. \right\}. \tag{8.4}
\end{aligned}$$

As being showed above, only  $F_2^{V,a}$  and  $G_2^{V,a}$  get contribution from  $ieQ_V a F^{\mu\nu} V_\mu^+ V_\nu^-$  which corresponds to the tree-level magnetic dipole moment, and for renormalization  $F_2^{V,a}, G_2^{V,a}$ , set  $a = 1$ .

## 2. Diagram b

- Dirac form factor

$$\begin{aligned}
F_1^{V,b} = & \frac{eQ_l}{2(m_1 - m_2)m_V^2} \left\{ (V_{ik}^R V_{jk}^{*L} + V_{ik}^L V_{jk}^{*R}) m_k \left[ (m_1^2 - 4m_V^2) B_0^{V,b} + 2m_1^2 B_1^{V,b} + \right. \right. \\
& m_1^2 B_{11}^{V,b} + 4B_{00}^{V,b} + \frac{1}{6} (m_1^2 - 3m_k^2 + 15m_V^2) \left. \right] - (V_{ik}^L V_{jk}^{*L} + V_{ik}^R V_{jk}^{*R}) m_1 \left[ (m_1^2 + 2m_V^2) B_1^{V,b} + \right. \\
& 2m_1^2 B_{11}^{V,b} + m_1^2 B_{111}^{V,b} + 8B_{00}^{V,b} + 6B_{001}^{V,b} + \frac{1}{12} (3m_1^2 - 10m_k^2 + 4m_V^2) \left. \right] \left. \right\}. \tag{8.5}
\end{aligned}$$

- Anapole form factor

$$\begin{aligned}
G_1^{V,b} = & \frac{eQ_l}{2(m_1 + m_2)m_V^2} \left\{ (V_{ik}^R V_{jk}^{*L} - V_{ik}^L V_{jk}^{*R}) m_k \left[ (m_1^2 - 4m_V^2) B_0^{V,b} + 2m_1^2 B_1^{V,b} + \right. \right. \\
& m_1^2 B_{11}^{V,b} + 4B_{00}^{V,b} + \frac{1}{6} (m_1^2 - 3m_k^2 + 15m_V^2) \left. \right] - (V_{ik}^L V_{jk}^{*L} - V_{ik}^R V_{jk}^{*R}) m_1 \left[ (m_1^2 + 2m_V^2) B_1^{V,b} + \right. \\
& \left. \left. 2m_1^2 B_{11}^{V,b} + m_1^2 B_{111}^{V,b} + 8B_{00}^{V,b} + 6B_{001}^{V,b} + \frac{1}{12} (3m_1^2 - 10m_k^2 + 4m_V^2) \right] \right\}.
\end{aligned} \tag{8.6}$$

### 3. Diagram c

- Dirac form factor

$$\begin{aligned}
F_1^{V,c} = & \frac{eQ_l}{2(m_2 - m_1)m_V^2} \left\{ (V_{ik}^R V_{jk}^{*L} + V_{ik}^L V_{jk}^{*R}) m_k \left[ (m_2^2 - 4m_V^2) B_0^{V,c} + 2m_2^2 B_1^{V,c} + \right. \right. \\
& m_2^2 B_{11}^{V,c} + 4B_{00}^{V,c} + \frac{1}{6} (m_2^2 - 3m_k^2 + 15m_V^2) \left. \right] - (V_{ik}^L V_{jk}^{*L} + V_{ik}^R V_{jk}^{*R}) m_2 \left[ (m_2^2 + 2m_V^2) B_1^{V,c} + \right. \\
& \left. \left. 2m_2^2 B_{11}^{V,c} + m_2^2 B_{111}^{V,c} + 8B_{00}^{V,c} + 6B_{001}^{V,c} + \frac{1}{12} (3m_2^2 - 10m_k^2 + 4m_V^2) \right] \right\}.
\end{aligned} \tag{8.7}$$

- Anapole form factor

$$\begin{aligned}
G_1^{V,c} = & \frac{-eQ_l}{2(m_2 + m_1)m_V^2} \left\{ (V_{ik}^R V_{jk}^{*L} - V_{ik}^L V_{jk}^{*R}) m_k \left[ (m_2^2 - 4m_V^2) B_0^{V,c} + 2m_2^2 B_1^{V,c} + \right. \right. \\
& m_2^2 B_{11}^{V,c} + 4B_{00}^{V,c} + \frac{1}{6} (m_2^2 - 3m_k^2 + 15m_V^2) \left. \right] + (V_{ik}^L V_{jk}^{*L} - V_{ik}^R V_{jk}^{*R}) m_2 \left[ (m_2^2 + 2m_V^2) B_1^{V,c} + \right. \\
& \left. \left. 2m_2^2 B_{11}^{V,c} + m_2^2 B_{111}^{V,c} + 8B_{00}^{V,c} + 6B_{001}^{V,c} + \frac{1}{12} (3m_2^2 - 10m_k^2 + 4m_V^2) \right] \right\}.
\end{aligned} \tag{8.8}$$

### 4. Diagram d

- Dirac form factor

$$\begin{aligned}
F_1^{V,d} = \frac{eQ_k}{2m_V^2} & \left\{ (V_{ik}^R V_{jk}^{*L} + V_{ik}^L V_{jk}^{*R}) (m_1 + m_2) m_k \left[ -4m_V^2 \sum_{i=0}^2 C_i^{V,d} + 4C_{00}^{V,d} + 6 \sum_{i=1}^2 C_{00i}^{V,d} + \right. \right. \\
& \sum_{i,j=1}^2 \frac{m_1^2 m_2^2}{m_i^2} \left( C_{ij}^{V,d} + \sum_{k=1}^2 C_{ijk}^{V,d} \right) - \frac{1}{6} \Big] + (V_{ik}^L V_{jk}^{*L} + V_{ik}^R V_{jk}^{*R}) \left[ \frac{1}{24} (7m_1^2 + 7m_2^2 + 12m_1 m_2 - \right. \\
& 28m_k^2 + 28m_V^2) + 2m_V^2 \sum_{i=0}^2 \left( \frac{(i-1)(i-2)}{2} (m_k^2 - m_1 m_2) + 2m_1 m_2 \right) C_i^{V,d} - \\
& 2(m_1 m_2 + m_k^2 + 2m_V^2) C_{00}^{V,d} + 12 \sum_{i=1}^2 \frac{m_1^2 m_2^2}{m_i^2} \left( C_{00i}^{V,d} + \sum_{j=1}^2 C_{00ij}^{V,d} \right) + \\
& \left. \left. \sum_{i,j=1}^2 \left[ m_1 m_2 (m_k^2 + 2m_V^2) + \frac{m_1^4 m_2^4}{m_i^2 m_j^2} \right] C_{ij}^{V,d} + \sum_{i,j,k=1}^2 \frac{m_1^4 m_2^4}{m_i^2 m_j^2} \left( C_{ijk}^{V,d} + \sum_{l=1}^2 C_{ijkl}^{V,d} \right) + 24C_{0000}^{V,d} \right] \right\}. \tag{8.9}
\end{aligned}$$

• Anapole form factor

$$\begin{aligned}
G_1^{V,d} = \frac{eQ_k}{2m_V^2} & \left\{ (V_{ik}^R V_{jk}^{*L} - V_{ik}^L V_{jk}^{*R}) (m_1 - m_2) m_k \left[ -4m_V^2 \sum_{i=0}^2 C_i^{V,d} + 4C_{00}^{V,d} + 6 \sum_{i=1}^2 C_{00i}^{V,d} + \right. \right. \\
& \sum_{i,j=1}^2 \frac{m_1^2 m_2^2}{m_i^2} \left( C_{ij}^{V,d} + \sum_{k=1}^2 C_{ijk}^{V,d} \right) - \frac{1}{6} \Big] + (V_{ik}^R V_{jk}^{*R} - V_{ik}^L V_{jk}^{*L}) \left[ \frac{1}{24} (-3m_1^2 - 3m_2^2 + \right. \\
& 12m_1 m_2 + 28m_k^2 - 28m_V^2) + 2m_V^2 \sum_{i=0}^2 \left( \frac{(1-i)(i-2)}{2} (m_k^2 + m_1 m_2) + 2m_1 m_2 \right) C_i^{V,d} + \\
& 2(-m_1 m_2 + m_k^2 + 2m_V^2) C_{00}^{V,d} - 12 \sum_{i=1}^2 \frac{m_1^2 m_2^2}{m_i^2} \left( C_{00i}^{V,d} + \sum_{j=1}^2 C_{00ij}^{V,d} \right) + \\
& \left. \left. \sum_{i,j=1}^2 \left( m_1 m_2 (m_k^2 + 2m_V^2) - \frac{m_1^4 m_2^4}{m_i^2 m_j^2} \right) C_{ij}^{V,d} - \sum_{i,j,k=1}^2 \frac{m_1^4 m_2^4}{m_i^2 m_j^2} \left( C_{ijk}^{V,d} + \sum_{l=1}^2 C_{ijkl}^{V,d} \right) - 24C_{0000}^{V,d} \right] \right\}. \tag{8.10}
\end{aligned}$$

• MDM form factor

$$\begin{aligned}
F_2^{V,d} = \frac{eQ_k}{2m_V^2} & \left\{ (V_{ik}^R V_{jk}^{*L} + V_{ik}^L V_{jk}^{*R}) m_k \left[ 4m_V^2 \sum_{i=0}^2 C_i^{V,d} + 4C_{00}^{V,d} + \sum_{ij=1}^2 \left( m_1 m_2 - \frac{m_1^2 m_2^2}{m_i^2} \right) C_{ij}^{V,d} - \right. \right. \\
& 6 \sum_{i=1}^2 C_{00i}^{V,d} - \sum_{i,j,k=1}^2 \frac{m_1^2 m_2^2}{m_i^2} C_{ijk}^{V,d} - \frac{1}{3} \Big] + (V_{ik}^L V_{jk}^{*L} + V_{ik}^R V_{jk}^{*R}) \left[ -m_V^2 \sum_{i=1}^2 \left( 4 \frac{m_1 m_2}{m_i} + 2m_i \right) C_i^{V,d} - \right. \\
& 2m_V^2 (m_1 + m_2) C_0^{V,d} + \sum_{i,j=1}^2 \left( -\frac{m_1 m_2}{m_i} (m_k^2 + 2m_V^2) + \frac{m_1^2 m_2^2}{m_i^2} m_j \right) C_{ij}^{V,d} + 2(m_1 + m_2) C_{00}^{V,d} + \\
& \left. \left. \sum_{i,j,k=1}^2 \frac{m_1^2 m_2^2}{m_j^2} m_i C_{ijk}^{V,d} + 6 \sum_{i=1}^2 m_i C_{00i}^{V,d} + \frac{m_1 + m_2}{6} \right] \right\}. \tag{8.11}
\end{aligned}$$

- EDM form factor

$$\begin{aligned}
G_2^{V,d} = \frac{eQ_k}{2m_V^2} & \left\{ (V_{ik}^L V_{jk}^{*R} - V_{ik}^R V_{jk}^{*L}) m_k \left[ 4m_V^2 \sum_{i=0}^2 C_i^{V,d} - 4C_{00}^{V,d} + \sum_{ij=1}^2 \left( m_1 m_2 - \frac{m_1^2 m_2^2}{m_i^2} \right) C_{ij}^{V,d} - \right. \right. \\
& 6 \sum_{i=1}^2 C_{00i}^{V,d} + \sum_{i,j,k=1}^2 \frac{m_1^2 m_2^2}{m_i^2} C_{ijk}^{V,d} + \frac{1}{3} \left. \right] + (V_{ik}^R V_{jk}^{*R} - V_{ik}^L V_{jk}^{*L}) \left[ -m_V^2 \sum_{i=1}^2 \left( 4 \frac{m_1 m_2}{m_i} - 2m_i \right) C_i^{V,d} - \right. \\
& 2m_V^2 (m_1 - m_2) C_0^{V,d} - \sum_{i,j=1}^2 (-1)^i \left( \frac{m_1 m_2}{m_i} (m_k^2 + 2m_V^2) + \frac{m_1^2 m_2^2}{m_i^2} m_j \right) C_{ij}^{V,d} + 2(m_1 - m_2) C_{00}^{V,d} - \\
& \left. \left. \sum_{i,j,k=1}^2 (-1)^i \frac{m_1^2 m_2^2}{m_j^2} m_i C_{ijk}^{V,d} - 6 \sum_{i=1}^2 (-1)^i m_i C_{00i}^{V,d} + \frac{m_1 - m_2}{6} \right] \right\}.
\end{aligned} \tag{8.12}$$

### 8.1.2 Charged scalar form factor

#### 1. Diagram a

- Dirac form factor

$$\begin{aligned}
F_1^{\phi,a} = \frac{eQ_\phi}{2} & \left\{ (Y_{ik}^R Y_{jk}^{*L} + Y_{ik}^L Y_{jk}^{*R}) (m_1 + m_2) m_k \sum_{i=0}^2 C_i^{\phi,a} - \right. \\
& (Y_{ik}^L Y_{jk}^{*L} + Y_{ik}^R Y_{jk}^{*R}) \left[ (m_1 + m_2) \sum_{i,j=1}^2 \frac{m_1 m_2}{m_i} \left( \frac{C_i^{\phi,a}}{2} + C_{ij}^{\phi,a} \right) + 2C_{00}^{\phi,a} \right] \left. \right\}.
\end{aligned} \tag{8.13}$$

- Anapole form factor

$$\begin{aligned}
G_1^{\phi,a} = \frac{eQ_\phi}{2} & \left\{ (Y_{ik}^L Y_{jk}^{*R} - Y_{ik}^R Y_{jk}^{*L}) (m_1 - m_2) m_k \sum_{i=0}^2 C_i^{\phi,a} + \right. \\
& (Y_{ik}^L Y_{jk}^{*L} - Y_{ik}^R Y_{jk}^{*R}) \left[ \sum_{i,j=1}^2 \left( \frac{m_1^2 m_2^2}{m_i^2} - m_1 m_2 \right) \left( \frac{C_i^{\phi,a}}{2} + C_{ij}^{\phi,a} \right) + 2C_{00}^{\phi,a} \right] \left. \right\}.
\end{aligned} \tag{8.14}$$

- MDM form factor

$$\begin{aligned}
F_2^{\phi,a} = \frac{eQ_\phi}{2} & \left[ (Y_{ik}^L Y_{jk}^{*L} + Y_{ik}^R Y_{jk}^{*R}) \sum_{i,j=1}^2 \frac{m_1 m_2}{m_i} \left( \frac{C_i^{\phi,a}}{2} + C_{ij}^{\phi,a} \right) - \right. \\
& \cdot (Y_{ik}^R Y_{jk}^{*L} + Y_{ik}^L Y_{jk}^{*R}) m_k \sum_{i=0}^2 C_i^{\phi,a} \left. \right].
\end{aligned} \tag{8.15}$$

- EDM form factor

$$G_2^{\phi,a} = \frac{eQ_\phi}{2} \left[ (Y_{ik}^L Y_{jk}^{*L} - Y_{ik}^R Y_{jk}^{*R}) \sum_{i,j=1}^2 (-1)^i \frac{m_1 m_2}{m_i} \left( \frac{C_i^{\phi,a}}{2} + C_{ij}^{\phi,a} \right) + \right. \\ \left. (Y_{ik}^L Y_{jk}^{*R} - Y_{ik}^R Y_{jk}^{*L}) m_k \sum_{i=0}^2 C_i^{\phi,a} \right]. \quad (8.16)$$

## 2. Diagram b

- Dirac form factor

$$F_1^{\phi,b} = \frac{eQ_l}{2(m_1 - m_2)} \left[ m_k (Y_{ik}^R Y_{jk}^{*L} + Y_{ik}^L Y_{jk}^{*R}) B_0^{\phi,b} - m_1 (Y_{ik}^L Y_{jk}^{*L} + Y_{ik}^R Y_{jk}^{*R}) B_1^{\phi,b} \right]. \quad (8.17)$$

- Anapole form factor

$$G_1^{\phi,b} = \frac{-eQ_l}{2(m_1 + m_2)} \left[ m_k (Y_{ik}^R Y_{jk}^{*L} - Y_{ik}^L Y_{jk}^{*R}) B_0^{\phi,b} - m_1 (Y_{ik}^L Y_{jk}^{*L} - Y_{ik}^R Y_{jk}^{*R}) B_1^{\phi,b} \right]. \quad (8.18)$$

## 3. Diagram c

- Dirac form factor

$$F_1^{\phi,c} = \frac{-e}{2(m_2 - m_1)} \left[ m_k (Y_{ik}^R Y_{jk}^{*L} + Y_{ik}^L Y_{jk}^{*R}) B_0^{\phi,c} - m_2 (Y_{ik}^L Y_{jk}^{*L} + Y_{ik}^R Y_{jk}^{*R}) B_1^{\phi,c} \right]. \quad (8.19)$$

- Anapole form factor

$$G_1^{\phi,c} = \frac{-e}{2(m_2 + m_1)} \left[ m_k (Y_{ik}^R Y_{jk}^{*L} - Y_{ik}^L Y_{jk}^{*R}) B_0^{\phi,c} + m_2 (Y_{ik}^L Y_{jk}^{*L} - Y_{ik}^R Y_{jk}^{*R}) B_1^{\phi,c} \right]. \quad (8.20)$$

## 4. Diagram d

- Dirac form factor

$$F_1^{\phi,d} = \frac{eQ_k}{2} \left\{ (Y_{ik}^R Y_{jk}^{*L} + Y_{ik}^L Y_{jk}^{*R}) (m_1 + m_2) m_k \sum_{i=0}^2 C_i^{\phi,d} + \right. \\ \left. (Y_{ik}^L Y_{jk}^{*L} + Y_{ik}^R Y_{jk}^{*R}) \left[ (m_1 m_2 + m_k^2) C_0^{\phi,d} + m_1 m_2 \sum_{i,j=1}^2 (C_i^{\phi,d} + C_{ij}^{\phi,d}) - 2C_{00}^{\phi,d} + \frac{1}{2} \right] \right\}. \quad (8.21)$$



- Anapole form factor

$$G_1^{\phi,d} = \frac{eQ_k}{2} \left\{ (Y_{ik}^L Y_{jk}^{*R} - Y_{ik}^R Y_{jk}^{*L}) (m_1 - m_2) m_k \sum_{i=0}^2 C_i^{\phi,d} + \right. \\ \left. (Y_{ik}^R Y_{jk}^{*R} - Y_{ik}^L Y_{jk}^{*L}) \left[ (m_k^2 - m_1 m_2) C_0^{\phi,d} - m_1 m_2 \sum_{i,j=1}^2 (C_i^{\phi,d} + C_{ij}^{\phi,d}) - 2C_{00}^{\phi,d} + \frac{1}{2} \right] \right\}. \quad (8.22)$$

- MDM form factor

$$F_2^{\phi,d} = \frac{-eQ_k}{2} \left[ (Y_{ik}^L Y_{jk}^{*L} + Y_{ik}^R Y_{jk}^{*R}) \sum_{i,j=1}^2 \frac{m_1 m_2}{m_i} \left( \frac{C_i^{\phi,d}}{2} + C_{ij}^{\phi,d} \right) + \right. \\ \left. (Y_{ik}^R Y_{jk}^{*L} + Y_{ik}^L Y_{jk}^{*R}) m_k \sum_{i=1}^2 C_i^{\phi,d} \right]. \quad (8.23)$$

- EDM form factor

$$G_2^{\phi,d} = \frac{-eQ_k}{2} \left[ (-Y_{ik}^L Y_{jk}^{*L} - Y_{ik}^R Y_{jk}^{*R}) \sum_{i,j=1}^2 (-1)^i \frac{m_1 m_2}{m_i} \left( \frac{C_i^{\phi,d}}{2} + C_{ij}^{\phi,d} \right) + \right. \\ \left. (Y_{ik}^R Y_{jk}^{*L} - Y_{ik}^L Y_{jk}^{*R}) m_k \sum_{i=1}^2 C_i^{\phi,d} \right]. \quad (8.24)$$

## 8.2 Fierz transformation

Fierz transformation is a mathematical tool used in quantum field theory and particle physics to rearrange or transform complex field operator's products into a more manageable form. This rearrangement is particularly useful when dealing with four-fermion interactions. Its core transformation is the Fierz identity. This identity allows the rearrangement of bilinear products of spinor fields. A bilinear product involves two spinor fields and gamma matrices. The Fierz identity expresses a product of two such bilinears in terms of a sum of bilinears with the spinor fields rearranged. In this study, the Fierz identity is formulated for the set

of gamma matrices  $\{\Gamma_S = 1, \Gamma_V = \gamma_\mu, \Gamma_T = \sigma_{\mu\nu}, \Gamma_A = \gamma_\mu \gamma_5, \Gamma_P = \gamma_5\}$ .

$$\sum_{\alpha} g_{\alpha} \bar{\psi}_i \Gamma_{\alpha} \psi_j \bar{\psi}_m \Gamma_{\alpha} \psi_n = \sum_{\beta} \tilde{g}_{\beta} \bar{\psi}_i \Gamma_{\beta} \psi_n \bar{\psi}_m \Gamma_{\beta} \psi_j \quad (8.25)$$

by a transformation matrix between  $g_{\alpha}$  and  $\tilde{g}_{\beta}$  that one can read off for  $\alpha, \beta$  running over the set  $\{S, V, T, A, P\}$

$$\begin{bmatrix} \tilde{g}_S \\ \tilde{g}_V \\ \tilde{g}_T \\ \tilde{g}_A \\ \tilde{g}_P \end{bmatrix} = \frac{1}{4} \begin{pmatrix} 1 & 4 & 12 & -4 & 1 \\ 1 & -2 & 0 & -2 & -1 \\ \frac{1}{2} & 0 & -2 & 0 & \frac{1}{2} \\ -1 & -2 & 0 & -2 & 1 \\ 1 & -4 & 12 & 4 & 1 \end{pmatrix} \begin{bmatrix} g_S \\ g_V \\ g_T \\ g_A \\ g_P \end{bmatrix} \quad (8.26)$$

where  $i, j, m, n$  are flavor indices.

### 8.3 Full massive Lorenz index two-body phase pace

The massive two-body phase space is useful to study the effect of Dirac and Majorana neutrino. Considering  $k, p$  are 4-momentum neutrinos, and the exchange momentum

$$q^2 = m_{\mu}^2 + m_e^2 - 2m_{\mu}E_e = 2m_{\mu} \left( \frac{m_{\mu}^2 + m_e^2}{2m_{\mu}} - E_e \right) = 2m_{\mu} (W - E_e). \quad (8.27)$$

The exchange energy minimum must be the total mass of neutrinos, therefore,

$$E_e^{max} = W - \frac{(m_k + m_p)^2}{2m_{\mu}}. \quad (8.28)$$

The massive two-body phase spaces then are written down in terms of

$$I^{\alpha\beta} = \int \frac{d^3k}{E_k} \frac{d^3p}{E_p} \delta^4(q - p - k) k^\alpha p^\beta = A^{3/2} \frac{\pi}{6} q^2 g_{\alpha\beta} + B A^{1/2} \frac{\pi}{3} q_\alpha q_\beta \quad (8.29)$$

$$I_{k(p)}^\alpha = \int \frac{d^3k}{E_k} \frac{d^3p}{E_p} \delta^4(q - p - k) k^\alpha (p^\alpha) = \pi \left( 1 \mp \frac{\Delta}{q^2} \right) q^\alpha \quad (8.30)$$

$$I = \int \frac{d^3k}{E_k} \frac{d^3p}{E_p} \delta^4(q - p - k) = 2\pi A^{1/2}, \quad (8.31)$$

where

$$A = 1 - \frac{2\Sigma}{q^2} + \frac{\Delta^2}{q^4} \quad (8.32)$$

$$B = 1 + \frac{\Sigma}{q^2} - \frac{2\Delta^2}{q^4} \quad (8.33)$$

$$\Sigma = m_k^2 + m_p^2 \quad (8.34)$$

$$\Delta = m_p^2 - m_k^2. \quad (8.35)$$



# Bibliography

- [1] L. Michel, *Interaction between four half spin particles and the decay of the  $\mu$  meson*, *Proc. Phys. Soc. A* **63** (1950) 514.
- [2] T. Kinoshita and A. Sirlin, *Polarization of electrons in muon decay with general parity-nonconserving interactions*, *Phys. Rev.* **108** (1957) 844.
- [3] A. Crivellin, M. Hoferichter and C. A. Manzari, *Fermi constant from muon decay versus electroweak fits and cabibbo-kobayashi-maskawa unitarity*, *Physical Review Letters* **127** (2021) .
- [4] T. Kinoshita and A. Sirlin, *Muon decay with parity nonconserving interactions and radiative corrections in the two-component theory*, *Phys. Rev.* **107** (1957) 593.
- [5] MUON G-2 COLLABORATION collaboration, *Final report of the e821 muon anomalous magnetic moment measurement at bnl*, *Phys. Rev. D* **73** (2006) 072003.
- [6] M. Steinhauser, *Übungen zu strahlungskorrekturen in eichtheorien, II*.  
*Institut für Theoretische Physik, Universität Hamburg, 22761 Hamburg*  
(2003) .
- [7] C. Bouchiat and L. Michel, *Theory of  $\mu$ -meson decay with the hypothesis of nonconservation of parity*, *Phys. Rev.* **106** (1957) 170.

- [8] A. Denner, *Techniques for the calculation of electroweak radiative corrections at the one-loop level and results for w-physics at lep200*, 2007.
- [9] L. Duc Truyen, *Electron muon elastic scattering in one-loop qed with soft-photon corrections*, 2020. 10.13140/RG.2.2.33520.48641.
- [10] T. D. Lee and C. N. Yang, *Theory of charged vector mesons interacting with the electromagnetic field*, *Phys. Rev.* **128** (1962) 885.
- [11] W. J. Marciano, *Fermi constants and “new physics”*, *Physical Review D* **60** (1999) .
- [12] T. Aoyama, T. Kinoshita and M. Nio, *Theory of the Anomalous Magnetic Moment of the Electron*, *Atoms* **7** (2019) 28.
- [13] R. K. Barman, R. Dcruz and A. Thapa, *Neutrino masses and magnetic moments of electron and muon in the zee model*, *Journal of High Energy Physics* **2022** (2022) .
- [14] J. Heeck and A. Thapa, *Zee-model predictions for lepton flavor violation*, *Physics Letters B* **841** (2023) 137910.
- [15] T. A. Chowdhury, J. Heeck, A. Thapa and S. Saad, *w boson mass shift and muon magnetic moment in the zee model*, *Phys. Rev. D* **106** (2022) 035004.
- [16] D. Chowdhury and O. Eberhardt, *Update of global two-higgs-doublet model fits*, *Journal of High Energy Physics* **2018** (2018) .
- [17] J. Bernon, J. F. Gunion, H. E. Haber, Y. Jiang and S. Kraml, *Scrutinizing the alignment limit in two-higgs-doublet models:  $m_h = 125$  GeV*, *Phys. Rev. D* **92** (2015) 075004.

- [18] D. Bryman, V. Cirigliano, A. Crivellin and G. Inguglia, *Testing lepton flavor universality with pion, kaon, tau, and beta decays*, *Annual Review of Nuclear and Particle Science* **72** (2022) 69–91.
- [19] C. Jarlskog, *Commutator of the quark mass matrices in the standard electroweak model and a measure of maximal CP nonconservation*, *Phys. Rev. Lett.* **55** (1985) 1039.

